This manuscript is a pre-print that was submitted for publication in Cretaceous Research. It has undergone peer-review and the manuscript has been accepted for publication. Subsequent versions of this manuscript may have slightly different content. After production the final version of this manuscript will be available via the 'Peer-reviewed Publication DOI' link on the right-hand side of this webpage.

Author contact address: Tim L. Luber, tllu@equinor.com

A revised chronostratigraphic framework for the Aptian of the Essaouira-Agadir Basin, a candidate type section for the NW African Atlantic Margin.

Tim L. Luber[1], Luc G. Bulot[2, 1], Jonathan Redfern[1], Mohamed Nahim[3], Jason Jeremiah[4], Mike Simmons[5, 10], Stéphane Bodin[6], Camille Frau[7], Mike Bidgood[8], Moussa Masrour[9]

[1] University of Manchester, School of Earth and Environmental Sciences, North Africa Research Group, M13 9PL, Manchester, UK

[2] Aix Marseille Université, CNRS, IRD, Coll France, CEREGE, Aix-en-Provence, Site Saint-Charles - case 67 - 3, place Victor Hugo - 13331 Marseille cedex 3, France

[3] Office National des Hydrocarbures et des Mines (ONHYM), 34 Avenue Al Fadila, B.P. 8030 NU, Rabat, Morocco

[4] Golden Spike Geosolutions Ltd, SG2 9US, Stevenage, UK

[5] Halliburton, 97 Jubilee Avenue, Milton Park, Abingdon, OX14 4RW, UK

[6] Aarhus University, Department of Geoscience, 8000 Aarhus C, Denmark

[7] Groupement d'Intérêt Paléontologique, Science et Exposition, 60 bd Georges Richard, 83000 Toulon, France

[8] GSS (Geoscience) Ltd, 2 Meadows Drive, Oldmeldrum, Aberdeenshire, AB51 0GA, UK

[9] Université Ibn Zohr, Faculté des Sciences, Département de Géologie, Laboratoire de Géologie Appliquée et Géo-Environnement (LAGAGE), B.P 8106 Cité Dakhla, Agadir, Morocco

[10] The Natural History Museum, Cromwell Road, London, SW7 5BD, UK

Abstract

The Essaouira-Agadir Basin (EAB) of Morocco contains the most extensive exposure of Aptian to Lower Albian strata onshore the NW African Atlantic Margin. This paper documents the first high-resolution, multi-disciplinary stratigraphic approach for the Aptian to Lower Albian on the NW African Atlantic Margin. Previous biostratigraphic work almost exclusively relied on long-distance correlation of ammonoids to the Mediterranean – Caucasian Realm. Recent biostratigraphic work has questioned some of the previous interpretations, highlighting significant faunal endemism and complications with correlation to other key Aptian sections.

This study focuses on 5 key sections: Tiskatine, Id Amran, Assaka, and DSDP 416/370. Distribution of ammonoids, foraminifera, and calcareous nannofossils are reported from a bed-by-bed collection made at Tiskatine.

The analysis of foraminiferal and calcareous nannofossil assemblages enable correlation to standard zonation schemes; but also highlights the urgent need of revision and future work on the integration of these schemes across disciplines. The study, further, includes $\delta^{13}C_{carb}$, $\delta^{13}C_{org}$, and total organic carbon (TOC) data that is compared to reference material from the Vocontian Basin.

The combined litho-, bio-, chemo-, and sequence stratigraphic analysis establishes a robust chronostratigraphic framework for regional and super-regional correlations and a type section is proposed for the Aptian of NW Africa at Tiskatine.

Keywords: Foraminifera, Calcareous Nannofossils, Ammonoids, Carbon Isotopes, Integrated Stratigraphy, Sequence Stratigraphy, Aptian, Essaouira-Agadir Basin, Morocco, Atlantic Margin

1. Introduction

This multi-disciplinary stratigraphic study for the Aptian of NW Africa builds on the pioneering work of Kilian and Gentil (1906), Roch (1930) and Ambroggi (1963), which was focused on the bio- and lithostratigraphy of the Essaouira-Agadir Basin (EAB). Additional work in the basin was carried out by Rey et al. (1986, 1988) and Witam (1998), but none of these studies proposed a high-resolution biostratigraphic framework. Yamina et al. (2002) provided a preliminary account on the distribution of Aptian planktonic foraminifera in the Western High Atlas in Morocco, although this work lacked systematic descriptions or illustration. The work of Peybernes et al. (2013) has given some insight into ammonoid biostratigraphic distribution for the Aptian of the EAB, but the authors mainly compared their observations to the Standard Mediterranean Ammonite Scale (SMAS) of Reboulet et al. (2011, 2014), albeit highlighting the need for a local zonation scheme. This was addressed by Luber et al. (2017), who established a new ammonoid biostratigraphic framework for the EAB and selected Tiskatine as the type section for the Aptian in the west-central part of the basin, as initially suggested by Roch (1930). Two basin-wide hiatus were recognised spanning (*i*) the time equivalent of the middle part of the *D. forbesi* Zone to lower part of the *E. martini* Zone (SMAS), and (*ii*) the *H. jacobi* Zone and the lowermost part of the *L. tardefurcata* Zone (SMAS).

To support those findings, enable regional and super-regional correlations, and to build a robust bio-chronostratigraphic framework, this study presents an integrated stratigraphic approach for the Aptian of NW Africa. Excellent outcrop conditions at Tiskatine (Fig. 1) allow a bed-by-bed collection for combined ammonoid, calcareous nannofossil, and foraminiferal analysis, affording biostratigraphic calibration. This is integrated with chemostratigraphic data, including the first Aptian $\delta^{13}C_{carb}$ and $\delta^{13}C_{org}$ curves and total organic carbon (TOC) analysis for the onshore NW African Atlantic Margin. Two previously undocumented sections (Assaka and Id Amran) are described and are key in identifying local tectonic control on sequence development. The onshore sections are correlated to DSDP borehole 370, and a revised biostratigraphic analysis of the upper Barremian to Lower Albian is presented.

70 This work also addresses correlation to the South Provence and Vocontian basins, key
71 locations that establish the standard biostratigraphy of Mediterranean-Caucasian Subrealm *sensu*
72 Westermann (2000) via the SMAS (Bergen, 2000; Kennedy et al. 2000; Moullade et al. 2000;
73 Dauphin, 2002; Herrle and Mutterlose, 2003; Herrle et .al, 2004; Kuhnt and Moullade, 2007; Baudin
74 et al., 2008; Kennedy et al. 2014; Frau et al. 2015, 2017a-b).

75 **FIGURE 1: PREFERED PLACEMENT**

2. Regional Setting and Stratigraphy

During the Early Cretaceous the EAB was best described by a broad embayment, the "Atlas Gulf", above the Berriasian shelf opening out to the west into the proto-Atlantic (Behrens et al., 1978). Carbonate platform sedimentation that prevailed through most of the Jurassic continued into the earliest Cretaceous but was curtailed through flooding of the basin margin in the early Valanginian (Rey et al., 1988; Ettachfini et al., 1998). The EAB is limited to the north by the Meseta and the Jebilet, to the south by the Souss Basin and to the east by the Massif Ancien de Marrakech. The modern-day exposure of the Mesozoic succession in the EAB occurs mainly along E-W trending anticlines and synclines linked to the Late Cretaceous to Cenozoic Atlasic orogeny (Laville et al., 2004) and combined salt tectonics (Tari and Jabour, 2013).

This work focuses on the Aptian of the west-central EAB. Studied sections are located within the Tiskatine syncline north of the prominent Cap Ghir anticline (Fig. 1, additional information in supplementary data). The lithostratigraphic framework is shown in figure 2, and has been discussed in detail in Luber et al. (2017). During the late Barremian to early Aptian (equivalent to the upper Bouzergoun Fm.), the region experienced a significant regressive phase (Nouidar and Chellai, 2001) (Fig. 2) leading to widespread exposure. Later during the Aptian (uppermost Bouzergoun Fm. to Tamzergout Fm.), transgression led to the developed of shallow-marine to open-marine shelfal conditions (Butt, 1982). Early Aptian (*P. dechauxi* Zone and potentially older) shoreface to shallow shelf conditions (upper Bouzergoun to lower Tamzergout Fm.) were followed by late Aptian mid- to outer shelf conditions. The Aptian/Albian boundary is marked by an important regressive phase, followed by a return to shelfal conditions (Oued Tidzi Fm.) that persisted throughout the Early Albian (Butt, 1982; Rey et al., 1988).

FIGURE 2: PREFERED PLACEMENT

2.1 Studied Sections

*2.1.1 Tiskatine (Sample-prefix: **MTTK**)*

Lat.: 30.821463° Long.: -9.702555° (Tiskatine 1) and Lat.: 30.810477° Long.: -9.739966° (Tiskatine 2). A sedimentary log of the sections with field photographs of key intervals can be found in figure 3.

FIGURE 3: PREFERED PLACEMENT

*2.1.2 Id Amran (Sample-prefix: **MTIA**)*

Lat.: 30.796026° Long.: -9.571094°

A detailed log is presented in figure 4 and field photographs are shown in the supplementary data.

FIGURE 4: PREFERED PLACEMENT

*2.1.3 Assaka (Sample-prefix: **MTAS**)*

Lat.: 30.807297° Long.: -9.787837°

A detailed log of the section is shown in figure 5 and in the supplementary data.

FIGURE 5: PREFERED PLACEMENT

2.1.4 DSDP Well 370 and 416

DSDP 370 – Lat.: 32.837500° Long: -10.776000° / **DSDP 416 –** Lat.: 32.836300° Long: -10.801000°

To correlate the EAB outcrop stratigraphy offshore, the upper Barremian to Lower Albian strata of DSDP boreholes 370 and 416 were sampled for calcareous nannofossils (request number: 049055-IODP and 049614-IODP). A summary log from borehole 370 is shown in figure 6. For sedimentary descriptions of this interval see Meyer et al. (1978). DSDP 370 is located about 155 kilometres offshore the modern Moroccan coastline in a water depth of 4214 m (Fig.1). DSDP 416 is located 5 Km west of borehole 370.

FIGURE 6: PREFERED PLACEMENT

3. Methods

The lithostratigraphy, main depositional environments, and ammonoid biostratigraphy of the Tiskatine section have been described comprehensively by Luber et al. (2017). The Tiskatine section was sampled bed-by-bed for bio- and chemostratigraphic analysis. Most samples come from the Tamzergout Fm., with a few samples from the underlying Bouzergoun Fm. and the overlying Oued Tidzi Fm (Fig. 3). At the Id Amran and Assaka sections, key intervals were sampled for calcareous nannofossil analysis to support ammonite findings and extend observations made at Tiskatine. A list of all species recorded with primary citation information is presented in the supplementary data. New ammonoid findings, key foraminifera, and calcareous nannofossil species are fully illustrated for future reference.

3.1 Biostratigraphy

3.1.1 Foraminiferal Biostratigraphy

Planktonic foraminifera have long been known to have stratigraphic utility within the later Early Cretaceous (e.g. Moullade, 1966) with a series of evolutionary inceptions and extinctions forming the basis for a standard planktonic foraminiferal zonation (e.g. Caron, 1985; Robaszynski and Caron, 1995; Premoli Silva and Verga, 2004; Ogg and Hinnov, 2012) shown in figure 7.

FIGURE 7: PREFERED PLACEMENT

96 samples from the Tiskatine section were prepared using the standard methodology described by Armstrong and Brasier (2005). Microfossil recovery was good to very good (typically more than 100 and sometimes over 500 specimens) but variable. Preservation was generally good. Key specimens are illustrated in figures 8 and 9.

The taxa present comprise a diverse assemblage of calcareous and agglutinating benthonic foraminifera and planktonic foraminifera. Planktonic foraminifera often form 50% or more of the total assemblage. Notwithstanding considerable discussion of the taxonomy of Early Cretaceous planktonic foraminifera (BouDagher-Fadel et al., 1997; Moullade et al., 2002; Bellier and Moullade,

151 2002; Verga and Premoli Silva 2003a, b; Premoli Silva and Verga, 2004; Ando et al., 2013) and
152 remaining uncertainties regarding precise stratigraphic range, their fundamental stratigraphic utility
153 remains. The taxa are identifiable with reference to the extensive literature on age-equivalent
154 cosmopolitan, Mediterranean and North-West European material (e.g. Bartenstein and
155 Bettenstaedt, 1962; Damotte and Magniez-Jannin, 1973; Premoli Silva and Verga, 2004). The
156 identification of key planktonic foraminifera follows the taxonomy of Verga and Premoli Silva
157 (2003a, b) and Premoli Silva and Verga (2004). Although the nomenclature of zonation varies
158 between authors (e.g. use of *Hedbergella infracretacea* Zone or *Pseudoplanomalina cheniourensis*
159 Zone instead of *Hedbergella trocoidea* Zone), the basic series of defining events is well understood.
160 Direct calibration to other stratigraphic tools (e.g. the SMAS and carbon isotope record and hence
161 the chronostratigraphic standard) is still at a very preliminary stage and remains a subject of ongoing
162 research.

163 **FIGURE 8: PREFERED PLACEMENT**

164 **FIGURE 9: PREFERED PLACEMENT**

165 *3.1.2 Calcareous Nannofossil Biostratigraphy*

166 44 samples from the Tiskatine section were analysed via standard techniques described by
167 Bown and Young (1998) and the picking brush method of Jeremiah (1996). At Id Amran a total of 8
168 samples where analysed for calibration to ammonite-bearing layers and as infill where ammonite
169 recovery was poor or absent. Similarly, an infill sample was studied from Assaka. At DSDP boreholes
170 370 and 416, nineteen and 5 samples were investigated, respectively. Samples were analysed semi-
171 quantitatively, with the first 30 fields of view counted and the remaining slide scanned for rare
172 specimens. Key specimens are illustrated in figure 10.

173 The nannofossil biostratigraphy is described with reference to the Lower Cretaceous NC
174 zones of Roth (1978, 1983) and subzones after Bralower et al. (1993). The standard Aptian
175 nannofossil zonations are, however, in urgent need of revision. The nominate species utilised in the
176 cosmopolitan NC zonation (Roth 1978; Bralower et al., 1993) either show diachronism (FAD
177 *Prediscosphaera columnata* (Stover, 1966), figure 10), difficulty of identification (differentiation of
178 *Hayesites albiensis* Manivit, 1971 from *Hayesites irregularis* [Thierstein in Roth and Thierstein, 1972)]
179 or a sporadic Last Appearance Datum (LAD) [*Micrantholithus hoschulzii* (Reinhardt, 1966)].
180 Therefore, the calibration of nannofossil zones as shown in standard texts (e.g. Ogg and Hinnov,
181 2012) requires revision. Distribution charts for all sections are provided in the supplementary data.

182 **FIGURE 10: PREFERED PLACEMENT**

183

184 *3.1.3 Ammonite Biostratigraphy*

185 Bed-by-bed collections for ammonites were made from the Id Amran and Assaka section.
186 Key bio-events were compared to the local biostratigraphic scale and bio-events of the EAB
187 recognised by Luber et al. (2017). Key specimens are illustrated in figure 11 and 12.

188 **FIGURE 11: PREFERED PLACEMENT**

189 **FIGURE 12: PREFERED PLACEMENT**

190

3.2 Carbon Isotope Stratigraphy

75 bulk rock samples were analysed at Tiskatine. The material is almost exclusively composed of shelfal marls and limestones, with a few calcareous sandstones. The $\delta^{13}C$ analysis was performed at the Friedrich-Alexander Universität in Erlangen, Germany, using a Gasbench II connected to a ThermoFisher Delta V Plus mass spectrometer for carbonate $\delta^{13}C$ analyses and a Flash EA 2000 elemental analyser connected online to ThermoFinnigan Delta V Plus mass spectrometer for bulk organic matter $\delta^{13}C$ analyses. All values are reported in per mil relative to V-PDB. Sample preparation procedure and standards follow Bodin et al. (2017). Reproducibility for carbonate $\delta^{13}C$ was ±0.04, for $\delta^{18}O$ ±0.05, and for $\delta^{13}Corg$ ±0.07‰ (1σ).

FIGURE 13: PREFERED PLACEMENT

4. Results

4.1 Biostratigraphy of the Essaouira-Agadir Basin

Herein we discuss foraminifera and calcareous nannofossils data supplementing the biostratigraphic framework of Luber et al. (2017) at the Tiskatine section and additional data from the Id Amran and Assaka sections.

4.1.1 Foraminifera Biostratigraphy – Zonation and Key Events (Tiskatine Section)

Figure 13 shows the relative proportions of the three main types of foraminifera (agglutinating, calcareous benthic, and planktonic). Although planktonic foraminifera usually comprise the dominant component of the assemblages (50% or more of the total numbers), benthic foraminifera are also abundant and diverse. These include calcareous rotalid species and agglutinating species. Calcareous miliolids are very rare.

214

215 ***Globigerinelloides ferreolensis* Zone: samples MTTK 164 – MTTK 186**

216 **Definition:** This zone was defined by Moullade (1966) as the interval from the extinction of
217 *Leopoldina cabri* (Sigal, 1952) (= *Schackoina cabri*) to the inception of *Globigerinelloides algerianus*
218 Cushman and Ten Dam, 1948.

219 Whilst rare specimens of *Globigerinelloides ferreolensis* (Moullade, 1961) can be found
220 within the *L. cabri* Zone (Robaszynski and Caron, 1995; Verga and Premoli Silva, 2003b; Premoli Silva
221 and Verga, 2004), extinction of *L. cabri* and the inception of common *G. ferreolensis* can be
222 considered to be synchronous (Aguado et al., 1999; Moullade et al., 2002, 2005), so that the
223 inception of common *G. ferreolensis* is also an effective marker for the base of the zone. At Tiskatine
224 *G. ferreolensis* (Fig. 8.4-6) occurs almost at the base of the Tamzergout Fm. in sample **MTTK 164** (Fig.
225 13). The uppermost part of the zone contains forms transitional between *G. ferreolensis* and *G.*
226 *algerianus* (Fig. 8.7-8) as well as specimens of *Globigerinelloides barri* (Bolli, Loeblich and Tappan,
227 1957).

228

229 ***Globigerinelloides algerianus* Zone: samples MTTK 187 – MTTK 208**

230 **Definition:** This zone was defined by Moullade (1966) as encompassing the total range of the
231 nominate species (Fig. 8.9-11).

232 This occurs between beds **MTTK 187** and **MTTK 203** at Tiskatine. The top of the zone can be
233 extended to sample **MTTK 208** (Fig. 13) which contains *G. barri* (Fig. 8. 1-3), a species that does not
234 extend above the *G. algerianus* Zone. Although a range chart within Premoli Silva and Verga (2004)
235 shows a minute extension of *G. barri* above the *G. algerianus* Zone, Verga and Premoli Silva (2003a)
236 stated that "*Globigerinelloides barri* disappears at the top of the *Globigerinelloides algerianus* Zone".
237 The local inception of *Hedbergella trocoidea* (Gandolfi, 1942) occurs midway within this zone.

238

***Hedbergella trocoidea* - *Paraticinella bejaouensis* zones undifferentiated: samples MTTK 210 – MTTK 247**

Definition: The *Hedbergella trocoidea* Zone is, according to Sigal (1977), the interval from the extinction of *G. algerianus* to the inception of *Paraticinella bejaouensis* (Sigal, 1966). The *Paraticinella bejaouensis* Zone is defined (Robaszynski and Caron, 1995) as the total range of the nominate species.

Since *P. bejaouensis* (Fig. 9.1) does not definitely occur in our studied material (a questionable specimen occurs in sample **MTTK 247**), the interval above the *G. algerianus* Zone with planktonic foraminiferal recovery (samples **MTTK 210** – **MTTK 247**) must be assigned to an undifferentiated *H. trocoidea* – *P. bejaouensis* zones (Figs. 7, 13). This is supported by the presence of *Pseudoplanomalina cheniourensis* (Sigal, 1952) (Fig. 8.12-15), a species that ranges no higher than the lower part of the *P. bejaouensis* Zone (Moullade et al., 2002; Bellier and Moullade, 2002; Ando et al., 2013). Additional taxa include *G. ferreolensis* and *H. trocoidea* (Fig. 9.2-4), two species that range throughout the upper Aptian (Moullade et al., 2002). The name *P. bejaouensis* is retained for reference to the standard literature, although proposals exist to correct the name of this species and its nominate zone to *Paraticinella rohri* (Ando et al., 2013).

4.1.2 Calcareous Nannofossil Biostratigraphy – Zonation and Key Events (Tiskatine Section)

All samples analysed from the Bouzergoun Fm. proved barren of nannoplankton (**MTTK 160**-**MTTK 162**). The basal 0.5m (**MTTK 163** – **MTTK 164**) mudstone section of the Tamzergout Fm. yielded low diversity and abundance assemblages. Diversity and abundance markedly increases from sample **MTTK 165b** upwards.

Subzone NC7A: samples MTTK 163 – MTTK 239

Definition: Interval from FAD of *Eprolithus floralis* (Stradner, 1962) to LAD of *M. hoschulzii* (Bralower et al., 1993).

M. hoschulzii, the marker for NC7A is found sporadically throughout the Tamzergout Formation. **MTTK 239** (Fig. 13) is likely an artificial top due to the sporadic local range. A boreal marker, *Crucibiscutum bosunensis* Jeremiah, 2001 is recorded from the Tiskatine section. Its FO at Tiskatine is recorded from bed **MTTK 185b**. The acme of *C. bosunensis* is at bed **MTTK 239**. *Zebrashapka vanhintei* Covington and Wise, 1987 is found throughout the upper Aptian but does not range up into the Lower Albian. *Assipetra terebrodentarius youngii* Tremolada and Erba, 2002 is found sporadically throughout the Tiskatine section.

Holococcoliths are particularly prevalent in the Aptian Tiskatine section. In the lower beds (**MTTK 165b** – **MTTK 185a**) *Calculites dispar* Varol *in* Al-Rifaiy et al., 1990 (Fig. 10) predominates. From bed **MTTK 187** above *Orastrum perspicuum* Varol *in* Al-Rifaiy et al., 1990 (Fig. 10) dominates with *Owenia partitum* (Varol *in* Al-Rifaiy et al., 1990) also showing quantitative influxes between beds **MTTK 200** and **MTTK 218**.

Subzone NC8A: sample MTTK 249

Definition: Interval from FAD of *P. columnata* to FAD of *H. albiensis* (Bralower et. al., 1993)

Sample **MTTK 249** yields both the FO of NC8A marker *P. columnata* together with *Rhagodiscus achlyostaurion* (Hill, 1976) and records a quantitative acme of the predominantly boreal species *Repagulum parvidentatum* (Deflandre and Fert, 1954) (Fig. 10). Holococcoliths and nannoconids are rare compared to the underlying upper Aptian, diversity and abundance of the nannofloras reduced.

4.1.3 Ammonite Biostratigraphy (Id Amran Section)

Compared to the biostratigraphic framework of Luber et al. (2017) the following ammonoid bio-events are recognised:

- Bio-event 1: occurrence of *Procheloniceras dechauxi* (Kilian and Reboul, 1915) in **MTIA 84**
- Bio-event 2: peak of diversity dominated by *Colombiceras* and *Epicheloniceras* **MTIA 105**
- Bio-event 3: first occurrence (FO) of the endemic species "*Epicheloniceras*" *marocanus* (Roch, 1930) in **MTIA 106**
- Bio-event 5: peak of abundance of *Pseudoaustraliceras* in beds **MTIA 131** and **135**
- Bio-event 6: sudden mass occurrence of *Elsaisabellia* in bed **MTIA 15**

Two additional ammonoid faunas are recognized by comparison to the ammonoid succession at Tiskatine. In bed **MTIA 98** the assemblage is dominated by "*Prochelonicera*s" sp. nov. (Fig. 11.11-17), large ancyloceratids associated with *Deshayesites* aff. *callidiscus* Casey, 1961a (Fig. 11.1-2). Slightly above bed **MTIA 100** contains an abundant fauna dominated by *Dufrenoyia praedufrenoyi* Casey, 1964 *sensu* Dutour (2005) (Fig. 11.3-9) and the occurrence of *Toxoceratoides rochi* Casey, 1961b (Fig. 11.10) is noteworthy.

4.1.4 Calcareous Nannofossil Biostratigraphy (Id Amran Section)

NC6B: samples MTIA 89 – MTIA 95

The lowermost Aptian nannofloras (**MTIA 89 – 95**) investigated from Id Amran are extremely rich yielding *Diazomatolithus lehmanii* Noël, 1965 (Fig. 10), high relative abundances of *Cyclagelosphaera margerelii* Noël, 1965 (Fig. 10) and A*ssipetra terebrodentarius* (Applegate et al. in Covington and Wise, 1987) (Fig. 10), events all occurring below the FAD of *E. floralis*. At Id Amran a rich nannoconid association also occurs with the wide canal forms *Nannoconus circularis* Deres and Achéritéguy, 1980 (Fig. 10) and *Nannoconus vocontiensis* Deres and Achéritéguy, 1980 predominant. The assemblage in this interval indicates zone NC6B.

The *D. forbesi* zone dated deposits at Id Amran between **MTIA 89** and **MTIA 95** are

312 stratigraphically younger than the deposits immediately below the basal Albian unconformity at
313 DSDP 370 and 416A (see below). At DSPD 370 the samples also yield *Zeugrhabdotus scutula* (Bergen,
314 1994) (Fig. 10) a form characteristic of the lower part of zone NC6B (Fig. 6).
315
316 **NC7A: samples MTIA 104 – MTIA 151**

317 MTIA 104 yields the FAD of *E. floralis* together with the LAD of *N. circularis*. Additional
318 events include the occurrence of *C. bosunensis* and *M. hoschulzii* recorded from, **MTIA 151** and
319 **MTIA 153** (*E. tiskatinensis* Zone). Additionally, **MTIA 153** yielded common *C. bosunensis* and an
320 incursion of common *Z. vanhintei* (Fig. 10) *(E. tiskatinensis* Zone).
321
322 **NC8A: sample MTIA 156**

323 *P. columnata*, *R. achlyostaurion* and rare *C. bosunensis* are recorded from **MTIA 156**,
324 confirming a basal Albian age (NC8A).

325

326 *4.1.5 Ammonite Biostratigraphy (Assaka Section)*

327 The co-occurrence of *Epicheloniceras* and *Colombiceras* in **MTAS 121** indicates the lower
328 upper Aptian *C. tobleri* Zone and Subzone. The mass occurrence of *Epicheloniceras* in **MTAS 122**
329 suggests a similar age, even though the occurrence of elements from the "*E.*" *marocanus* Subzone
330 cannot be excluded. The fauna collected from **MTAS 123** contains reworked upper Aptian
331 ammonites from the *A. aschiltaensis* Zone [*Pseudoaustraliceras* gr. *ramososeptatum* (Anthula,
332 1900)], from the *E. tiskatinensis* Zone ["*Epicheloniceras*" gr. *clansayense* (Jacob, 1905)] together with
333 *Mellegueiceras* and "*Hypacanthoplites*" of the *paucicostatus* (Breistroffer in Dubourdieu, 1953)
334 group that are diagnostic of the Lower Albian (Latil, 2011; Luber et al., 2017). Key ammonoid
335 material is illustrated in figure 12.

336

337 *4.1.6 Calcareous Nannofossil Biostratigraphy (Assaka Section)*

338 **NC8A: sample MTAS 124**

339 An Early Albian age for **MTAS 124** is established by the co-occurrence of *P. columnata* and a
340 questionable specimen of *R. achlyostaurion*.

341

342 *4.1.7 Nannofossil Biostratigraphy DSDP Leg 41 borehole 370*

343 The following key bio-events have been recognised in the studied section (Fig. 6):

344 **NC6A**

345 • 1. LO of common nannoconids and *Micrantholithus obtusus* Stradner, 1963*;* presence of
346 *Flabellites oblongus* (Bukry, 1969) (Fig. 10) at 874.81m indicating an age no older than latest
347 Barremian (Zone NC6A).
348 • 2: *LO of Nannoconus steinmannii* Kamptner, 1931 (Fig. 10) at 873.98 m
349 • 3: LO of *Conusphaera rothii* (Thierstein, 1971) (Fig. 10) at 873.31m. In this study the LAD of *C.*
350 *rothii* is utilised as an approximation for top Barremian (Zone NC6A).

351 **NC6B**

352 • 4. LO of *Z. scutula* at 840.03 indicating an age no younger than earliest Aptian (Zone NC6B).
353 • 5: LO of HRA of *C. margerelii* with an influx of *A. terebrodentarius* and LO of consistent *P.*
354 *furtiva* in the absence of *E. floralis* indicating an age no younger than early Aptian intra *D.*
355 *forbesi* ammonite Zone equivalent age at 839.87m (Zone NC6B).

356 **NC8A**

357 • 6. FO of *R. achlyostaurion*, presence of *C. bosunensis* and *A. terebrodentarius youngii*
358 indicates a basal Albian age at 838.57m (Zone NC8A).
359 • 7. FO of *P. columnata* at 837.90m (Zone NC8A).

- 8. LO of *A. terebrodentarius youngii* at 835.95m (Zone NC8A). *A. terebrodentarius youngii* is more extensively recorded from the oceanic DSDP 370 than at the shallower shelf outcrop at Tiskatine, a result of this form's preference to deeper waters (Street and Bown, 2000).
- 9. FO of an influx of *R. parvidentatum* at 836.80 m.
- 10. LO of *C. bosunensis* at 830.89m (Zone NC8A).
- *C. bosunensis* is found from 830.89m down to the basal Albian sample analysed at 838.57m.

At the DSDP 370 borehole both *C. bosunensis* and *A. terebrodentarius youngii* are found to have LO's extending into the basal Albian.

4.1.8 Nannofossil Biostratigraphy DSDP Leg 41 borehole 416

The following key bio-events have been recorded in core 6-4 and 6 core catcher (CC):

- Lowermost Aptian sediments yielding abundant *A. terebrodentarius*, common *C. margerelii* and common *Z. scutula*, again in the absence of nannoconids (core 6 CC); lower part Zone NC6B.
- Lower Albian sediments yielding an influx of *R. parvidentatum*, abundant *R. achlyostaurion* and the presence of *P. columnata* (core 6 CC and 6-4); Zone NC8A.

4.2 Carbon Isotope Stratigraphy: $\delta^{13}C_{carb}$ and $\delta^{13}C_{org}$

The $\delta^{13}C_{carb}$ values of the Tiskatine section between **MTTK 163** and **MTTK 249** (Fig. 14) range between -0.34‰ (**MTTK 249**) and 1.9‰ (**MTTK 229**) and can be grouped into 5 major segments.

- **Segment 1**: Overall increase of $\delta^{13}C_{carb}$ values from -0.13‰ to 1.83 ‰ between **MTTK 163** to **MTTK 172**, with wide scatter of values between **MTTK 163** to **MTTK 169**.
- **Segment 2**: Decreasing trend of $\delta^{13}C_{carb}$ values following **MTTK 172** to 0.31‰ in **MTTK 185b**.
- **Segment 3**: Overall plateau of $\delta^{13}C_{carb}$ values from **MTTK 186** to **MTTK 206/208**, oscillating

between 0.29 (**MTTK 197**) and 1.32‰ (**MTTK 204**). A small long-term increasing trend can be observed within the segment. On top of segment 3, a short-lived negative excursion (from **MTTK 206** to **MTTK 213**) can be observed.

- **Segment 4**: Rapid increasing trend in $\delta^{13}C_{carb}$ values from **MTTK 213** to **MTTK 216** followed by an attenuated increase towards a maximum value in the section of 1.90‰ in **MTTK 229**.
- **Segment 5**: Pronounced decreasing trend of $\delta^{13}C_{carb}$ values following **MTTK 229** to the minimum value in the section of -0.34‰ in **MTTK 249**.

The $\delta^{13}C_{org}$ values of the Tiskatine section between **MTTK 160** and **MTTK 249** (Fig. 14) range between -27.27‰ (**MTTK 160**) and -22.49‰ (**MTTK 161)** and can be grouped into 4 major segments.

- **Segment 1**: Decreasing trend of $\delta^{13}C_{org}$ values from **MTTK 161** (-22.49‰) to -26.86‰ in **MTTK 186**.
- **Segment 2**: Overall plateau of $\delta^{13}C_{org}$ values from **MTTK 186** to **MTTK 206** (-26.5‰).
- **Segment 3**: Increasing values until **MTTK 226** (-25.21‰).
- **Segment 4**: Overall plateau until the basal Albian unconformity.

FIGURE 14: PREFERED PLACEMENT

5. Discussion

5.1 Biostratigraphy

5.1.1 Age interpretation - Foraminifera

All planktonic foraminifera present suggest a late Aptian age for the Tamzergout Fm. at Tiskatine (Fig. 7). Lower Aptian taxa, such as the distinctive *L. cabri*, are absent and the lowest significant planktonic foraminifera occurring in the section, *G. ferreolensis,* is restricted to the upper Aptian according to some authors (e.g. Moullade et al. 2002). The occurrence of this species in the highest part of the Tamzergout Fm. (Fig. 13) indicates a late Aptian age (along with the presence of

409 *H. trocoidea* and, just below these occurrences, *P. cheniourensis*) (Premoli Silva and Verga, 2004).
410 Taxa indicative of an Early Albian age such as *T. primula* are absent from the Tamzergout Fm. at
411 Tiskatine. Ammonoid and calcareous nannofossil occurrences demonstrate an Albian age for the
412 overlying Oued Tidzi Fm. This interpretation contrasts with that of Yamina et al. (2002) who
413 described, but did not illustrate, a variety of lower Aptian planktonic foraminiferas species from the
414 lower part of the Tamzergout Fm. at localities north of the Amsittene Anticline. The ammonoid work
415 of Luber et al. (2017) highlighted that the base of the Tamzergout Fm., as originally defined by
416 Duffaud et al. (1966) is markedly diachronous being the lower part of the lower Aptian at some
417 localities and lower upper Aptian at others (Fig. 2). A possibility to explain the discrepancies in age
418 interpretation, in addition to the difficulties in applying lithostratigraphy, is that the Tiskatine section
419 represents deposition in proximity of a local high, such that the well-established intra-Aptian hiatus
420 (sequence boundary) (Peybernes et al., 2013; Luber et al., 2017) is most expansive there.
421 The late Aptian age interpretation of the Tamzergout Fm. at Tiskatine provided by the
422 planktonic foraminifera is in broad agreement with the age interpretations provided here from the
423 occurrences of ammonoids and calcareous nannofossils (Fig. 13), as well as the stable carbon isotope
424 record (Fig. 14). It is very likely that the uppermost Aptian "*H*". *jacobi* Zone is missing in the Tiskatine
425 section as *P. cheniourensis* occurs near the top of the formation, a species with a LAD well below the
426 top of the Aptian or reported "uppermost Gargasian" (Moullade et al., 2002; Ando, et al., 2013).
427 Ammonoid, calcareous nannofossils, and carbon isotope records support this interpretation (Figs.
428 13, 14).
429 The calibration of the standard planktonic foraminiferal zonation to the SMAS is still in
430 progress as, regrettably, a limited number of publications document the co-occurrence of planktonic
431 foraminifera alongside ammonoid occurrences in the classic sections. The data from the Tiskatine
432 section may be very important in this respect as the local ammonoid zonation of Luber et al. (2017)
433 can be calibrated to the SMAS and the $\delta^{13}C$ record. Calcareous nannofossils provide additional
434 constraint.

435 The oldest ammonites found in the Tamzergout Fm. at Tiskatine are assigned to the *C.*
436 *tobleri* Zone. This is calibrated to a position midway within the *E. martini* Zone of the SMAS (Luber et
437 al., 2017). The recognition of the *G. ferreolensis* planktonic foraminiferal Zone for the same samples
438 is intriguing in that for some authors the *G. ferreolensis* Zone is regarded as occurring at the base of
439 the upper Aptian, in the lowest part of the *E. martini* Zone (Ogg and Hinnov, 2012). Our data would
440 suggest that positioning the base of *G. ferreolensis* Zone above the base of the upper Aptian, within
441 the *E. martini* Zone (Figs. 7, 13) would be preferable as indicated by Robaszynski and Caron (1995)
442 and Dauphin (2002). The $\delta^{13}C$ record points to calibration with the Ap9 segment of the standard $\delta^{13}C$
443 curve from the Vocontian Trough. Ap9 is low within the *E. martini* Zone and calibrates with the *G.*
444 *ferreolensis* Zone.
445 The local *A. aschiltaensis* ammonite Zone found in the middle part of the Tamzergout Fm. at
446 Tiskatine is calibrated (Luber et al., 2017) to straddling the upper *E. martini* to *P. melchioris* zones of
447 the SMAS. The portion of the Tiskatine section assigned to the *A. aschiltaensis* Zone is also assigned
448 to the *G. algerianus* planktonic foraminifera Zone and the upper part of the *G. ferreolensis* Zone.
449 Although these zones are calibrated by some authors to levels within the *E. martini* Zone (e.g. Ogg
450 and Hinnov, 2012) the data from Tiskatine (Figs. 13) would suggest that placement of the top of the
451 *G. algerianus* Zone extends to the *P. melchioris* Zone as suggested by Robaszynski and Caron (1995)
452 and Dauphin (2002).
453
454 *5.1.2 Age interpretation Ammonites and biostratigraphic correlation to the Standard Mediterranean*
455 *Scale (SMAS)*
456 A state of the art of the integrated ammonoid, planktonic foraminifera, and calcareous
457 nannofossil distribution in the reference sections of the South Provence and Vocontian basins are
458 presented in the supplementary data. These synthetic figures include both published (Bergen, 2000;
459 Kennedy et al., 2000, 2014; Moullade et al., 2000, 2005; Dauphin, 2002; Herrle and Mutterlose,
460 2003; Dutour, 2005; Kuhnt and Moullade, 2007; Frau et al., 2015) and unpublished data by two of us

(CF and LGB). The bio-events selected are the ones more reliable to correlate the EAB and the SMAS successions (Luber et al., 2017). Formal revision of the SMAS is far beyond the scope of the present contribution. This work is currently in progress and will be published elsewhere.

By comparison with the ammonoid successions of SE France the fauna from **MTIA 98** indicates the middle part of the *D. forbesi* Zone *sensu* Frau et al. (2015). The assemblage from **MTIA 100** is indicative of the middle part of the *D. furcata* Zone *sensu* Dutour (2005). Therefore, these two early Aptian ages demonstrate the existence of a hiatus that spans the upper part of the *D. forbesi* Zone, the *D. deshayesi* Zone and the lower part of the *D. furcata* Zone on top of bed **MTIA 98**. The hiatus includes the time equivalent of the OAE1a-related culmination and succeeding recovery. These ages are further supported by the occurrence of the calcareous nannofossil association of *E. floralis* and *N. circularis* in **MTIA 104** of latest early Aptian age.

As outlined by Luber et al. (2017) the lack of precise definition of the Aptian and Lower Albian biochrono-zones and subzones of the SMAS handicaps the correlation between the EAB and the SMAS. This point was already addressed by Owen (1996), Dauphin (2002), Bulot (2010), Bulot et al. (2014), Frau et al. (2015, 2016). Consequently, the high-resolution integrated stratigraphy of the Aptian stage is at a far more preliminary stage than advocated (see also discussions in Frau et al., 2018).

5.1.3 Age interpretation Calcareous Nannofossils

Tiskatine

NC7A: The LAD of *M. hoschulzii* has been conventionally calibrated (Bralower et al., 1993; Ogg and Hinnov, 2012) to a position slightly above the base of the upper Aptian, at a level close to the base of the *E. martini* Zone (SMAS). This conventional calibration for the top NC7A appears depressed to more recent records from northwestern Europe (Jeremiah, 2000, 2001), the Gulf of Mexico (Phelps et al., 2015; Supplementary document) and this study at Tiskatine (EAB). Here at Tiskatine *M. hoschulzii* ranges up to the local "*Hypacanthoplites*" spp. Subzone, correlated to the

upper part of the *A. nolani* Zone (Fig. 13). It is uncertain whether its LO at **MTTK 239** is its true LAD, or a result of truncation at the Aptian/Albian boundary unconformity above (Fig. 13). Regardless, the range of *M. hoschulzii* substantially extends the conventional LAD.

The occurrence of the boreal marker *C. bosunensis* is noteworthy at Tiskatine and could help establish a calibration datum between the Boreal and Tethyan realms. In the boreal North Sea, *C. bosunensis* has a short stratigraphic acme range constrained to the uppermost beds of the *E. martinoides* and *P. nutfieldensis* zones of early late Aptian age (Jeremiah, 2000). Its true LAD is more sporadic, with rare occurrences ranging up into the lowermost Albian of the North Sea (Jeremiah, 2001). Recent studies (Phelps et al., 2015; supplementary document) have shown a more extensive geographical distribution outside of the North Sea. At Tiskatine the acme of *C. bosunensis* is at bed **MTTK 239** (Fig. 13). This acme only 2 m below the Aptian/Albian boundary unconformity suggests that sediments equivalent to the uppermost Aptian *H. jacobi* Zone are extremely condensed or eroded. In the North Sea, *C. bosunensis* is only recorded rarely from *H. jacobi* dated sediments (Jeremiah, 2001; Jeremiah et al., 2010).

Further, it is noteworthy that the occurrence of *Z. vanhitei* in upper Aptian sediments (Fig. 13) extends the range of this form from its published LAD in the lower Aptian (Bown et al., 1998).

NC7B/NC7C: Subzones NC7B and NC7C are not utilised in the current study. These subzones are based on a differentiation of the FAD of *R. achlyostaurion* from that of the FAD of *P. columnata*. Current studies indicate that the base of *R. achlyostaurion* lies close to the base of the Albian where it appears together with *P. columnata* (Kennedy et al. 2000, 2014) as at Tiskatine (Fig. 13).

NC8A: There is a major nannofloral turnover at the Aptian/Albian boundary section at Tiskatine. The FO of abundant *R. parvidentatum* is a potentially important local correlative event marking the base of the Albian along the Moroccan Atlantic Margin, here occurring with the FAD of *R. achlyostaurion* and *P. columnata* (Sample **MTTK249**).

513

514 **Id Amran**

515 **NC6B:** Here the assemblage of **MTIA 89-95** is characteristic of other lower *D. forbesi* Zone
516 ammonite dated assemblages (Atherfield Clay, UK, Fischschiefer UK North Sea; Jeremiah, 2000;
517 Jeremiah et al., 2010; Lehmann et al., 2012, 2016).

518 **NC7A:** Sample MTIA 104 yields *E. floralis* and the LAD of *Nannoconus circularis*. The two
519 samples at **MTIA 151** and **MTIA 153** yield a Late Aptian assemblage reminiscent of equivalent
520 sediments investigated at Tiskatine. *M. hoschulzii, C. bosunensis* (common at **MTIA 153**), *Z. vanhintei*
521 and *A. terebrodentarius* ssp. *youngii* are all recorded.

522 **NC8A:** A sample from the base of the Oued Tidzi Formation (**MTIA 156**), above the
523 uppermost Aptian – basal Albian unconformity, yielded *P. columnata* and *R. achlyostaurion* together
524 with *C. bosunensis*. *R. parvidentatum* was not recorded in this sample. It appears that *C. bosunensis*
525 ranges into basal Albian deposits. The presence at Id Amran suggests that the lowermost Albian
526 deposits above the basal Albian unconformity are slightly older here than those preserved at
527 Tiskatine where the LAD of *C. bosunensis* is truncated. A more extensive sequence of events
528 including the Lower Albian LO (Last Occurrence) of *C. bosunensis* and *A. terebrodentarius youngii* is
529 recorded at DSDP 370 (see discussion below).

530

531 **DSDP 370/416**

532 **NC6A:** At DSDP 370 the exact boundary between the upper Barremian and lower Aptian can
533 not be determined based on the calcareous nannofossil data. It is either located at the erosive base
534 of the turbidity current in the upper part of core section 34-1 (872.85 – 873.26 m) above deposits of
535 NC6A, or located within the core gap above. The base of the turbidite at 873.26 m could correspond
536 to a regional regressive phase recognized at the Barremian - Aptian transition within the Bouzergoun
537 Fm. onshore the EAB.

538 **NC6B:** The basal part of core 32-4 (840.42 – 389.87 m) contains strata of early Aptian age.

These deposits are older than the sedimentary rocks assigned to NC6B from the Id Amran section onshore. Here at DSDP 370 the occurrence of *Z. scutula* indicates the lower part of NC6B.

NC7A: The recorded stratigraphy of NC7A, forming the bulk of the Tiskatine section, is not recorded at DSDP borehole 370.

NC8A: The contact between the lowermost Aptian (NC6B) and Lower Albian sequence (NC8A) lies between 838.57 – 839.87 m. Onshore in the EAB the Aptian/Albian boundary is marked by a regional erosive unconformity and a distinct colour change from blue-grey marls of the Tamzergout Formation to green marls of the Oued Tidzi Formation. This colour change is also observed in the core section 32-4 (838.57 – 839.87 m, Fig. 6). Therefore, a hiatus and the basal Albian unconformity are tentatively placed at the erosive contact at 839.68 m. It could also fall at the base of the erosive turbidite at 839.87 m. The boundary is thought to correlate to the regional sequence boundary recognized onshore (Luber et al., 2017) and in borehole 370 appears to erode most of the lower Aptian and all the upper Aptian strata.

At the adjacent DSDP Borehole 416A the basal Albian unconformity is also recorded within core 6 (CC). Here again, Lower Albian (NC8A) sediments rest directly with a marked hiatus upon lowermost Aptian sediments (NC6B).

5.2 Carbon Isotope Chemostratigraphic Correlation

This section provides interpretation of the $\delta^{13}C$ curve in the Tiskatine section and a correlation to the biostratigraphically well-constrained Vocontian basin (Fig. 15).

FIGURE 15: PREFERED PLACEMENT

5.2.1 Interpretation of the $\delta^{13}C$ trend in the Tiskatine section

To discuss our $\delta^{13}C$ dataset it must be assessed that local water cycling processes or diagenesis had no significant influence and the observed $\delta^{13}C$ trends are mainly representative of global change in the carbon cycle. The here-analysed carbonate samples are made of bulk micrite

565 deposited in an open shelf setting and open ocean water masses are expected (Immenhauser et al.,
566 2002). Resetting of δ^{13} C_{carb} values by late diagenetic processes are unlikely since the abundance of
567 carbonates act as a strong buffer against significant isotopic exchange with C-poor fluids (e.g.
568 Marshall, 1992). The absence of major diagenetic resetting of our δ^{13} C_{carb} dataset is confirmed by
569 measured values typical for an Aptian oceanic signature, as reported from numerous studies (e.g.
570 Herrle et al., 2004; Bodin et al., 2015). The values of the $\delta^{13}C_{org}$ dataset are similar to McAnena et al.
571 (2013) for DSDP borehole 545.

572 For the $\delta^{13}C_{carb}$ values, care must be taken for the lowermost (**MTTK 162** - **MTTK 169**) and
573 uppermost (**MTTK 237** - **MTTK 249**) parts of the Tamzergout Formation. Here high amplitude and
574 sharp fluctuation of $\delta^{13}C_{carb}$ values are observed. Since similar trends and fluctuations cannot be
575 observed in the $\delta^{13}C_{org}$ dataset, it can be hypothesized that these high-amplitude and sharp
576 fluctuations of $\delta^{13}C_{carb}$ values are linked to early diagenetic resetting. This is most notably close to
577 the hiatus separating the Tamzergout and Oued Tidzi Fms. The large negative C-isotope excursion at
578 the top of the Tamzergout Fm. resembles a negative excursion associated with subaerial exposure
579 diagenesis due to the adjunction of ^{13}C-depleted carbon derived from soil development (Allan and
580 Matthews, 1982). There is, however, no physical indication for subaerial exposure related to the
581 Lower Albian unconformity at the base of the Oued Tidzi Fm. Oxidation of marine organic matter or
582 local oceanographic conditions related to water masses isolation could thus be a more likely
583 explanation for these two negative excursions.

584

585 *5.2.2 Correlation to the South Provence and Vocontian Basin*

586 The chemostratigraphic correlation between the EAB and the SE France reference sections
587 established in the South Provence and Vocontian Basin (Herrle et al., 2004) has to take into account
588 the two basin-wide hiatus recognized in the Tiskatine section, covering 1) the upper *D. forbesi* Zone
589 to lower *E. martini* Zone and 2) the whole *H. jacobi* to lowermost *L. tardefurcata* Zone equivalent of
590 the SMAS. Furthermore, the sedimentary record in the EAB is far more condensed than its

591 counterparts in SE France (Fig.15).

592 Considering the hiatus in the EAB and stratigraphic gaps, the overall $\delta^{13}C_{org}$ curve as well as
593 the $\delta^{13}C_{carb}$ curve of the EAB (Fig. 14) matches the established curves of the Vocontian and South
594 Provence basins. The lowermost and uppermost part of the Tiskatine $\delta^{13}C_{carb}$ record cannot be
595 chemostratigraphically correlated to the French reference curve, which corroborates the hypothesis
596 of diagenetic alteration. Eliminating these data allows clear observation of an initial negative $\delta^{13}C$
597 trend (minimum amplitude of ca. 1‰ for the $\delta^{13}C_{carb}$ record, and 4‰ for the $\delta^{13}C_{org}$ record) that
598 correspond well to the upper part of the decline in $\delta^{13}C$ values spanning the lower – upper Aptian
599 transition observed in the Vocontian Basin (in both bulk micrite and belemnite records; Herrle et al.,
600 2004; Bodin et al., 2015), as well as in the South Provence Basin (Kuhnt et al., 2011) and elsewhere
601 (e.g. Menegatti et al., 1998; De Gea et al., 2003; Godet et al., 2014). This decline is a global
602 environmental signal, resulting from a return to pre-OAE 1a positive excursion values (C8 segment of
603 Menegatti et al., 1998; see also Bodin et al., 2015). Given that the C7 segment of Menegatti et al.
604 (1998), i.e. the maximum of the lower Aptian positive $\delta^{13}C$ (related to the OAE 1a), is not recorded in
605 Tiskatine, it is difficult to assess which exact part of the C8 segment of Menegatti et al. (1998) is
606 represented by the decreasing trend observed in our record. As the here observed decreasing trend
607 falls within the middle to upper *E. martini* Zone equivalent of SMAS, we correlate it to the upper part
608 of the C8 segment (Menegatti et al., 1998).

609 The following $\delta^{13}C$ plateau in the Tiskatine section (around 0.7‰ for $\delta^{13}C_{carb}$ and around -
610 26.5‰ for $\delta^{13}C_{org}$) can be correlated to the Ap10 and Ap11 segments of Herrle et al. (2004), spanning
611 most of the *G. algerianus* / *H. trocoidea* foraminifera zone. This agrees with our biostratigraphic
612 zonation. Lastly, the $\delta^{13}C$ positive excursion spanning the upper part of the Tiskatine section
613 (excluding the diagenetically altered uppermost part of the $\delta^{13}C_{carb}$ record) and the plateau of $\delta^{13}C_{org}$
614 in the uppermost part of the section correlates well to the Ap12 and Ap 13 segments of Herrle et al.
615 (2004), supporting the correlation between the *E*. *tiskatinensis* ammonite Zone in Morocco and the
616 *N. nolani* ammonite Zone in SE France (Luber et al., 2017).

Finally, it should be noted that the $\delta^{13}C_{org}$ value of -27.27‰ for the **MTTK 160** sample at the base of the section is similar to the $\delta^{13}C_{org}$ values observed within the lowermost *A. aschiltaensis* Zone. This is consistent with its earliest Aptian pre-OAE 1a age attribution (*P. dechauxi* Zone, which is the equivalent to the lower part of the *D. forbesi* Zone; Luber et al., 2017). Indeed, in SE France, similar $\delta^{13}C$ values have also been observed for these two intervals (Föllmi et al., 2006; Kuhnt et al., 2011; Bodin et al., 2013, 2015).

The comparison between carbonate and organic matter $\delta^{13}C$ records of the Tiskatine section (Fig. 14) and the Vocontian Basin reference section (Fig. 15) further supports the biostratigraphic scheme established in Morocco. Additionally, the correlation, additionally, confirms that key stratigraphic intervals, the OAE 1a-equivalent and the Aptian/Albian boundary section, are not recorded at Tiskatine.

5.3. The Evolution of the EAB during the Aptian

5.3.1 Depositonal Environment and Sequence Stratigraphic Interpretation

Through palaeontological and field observations, depositional environments and key sequence stratigraphic surfaces are described for the Tiskatine section (Fig. 13). Supporting observations come from the Id Amran and Assaka sections and information from the DSDP boreholes 370/416 is also discussed.

Three 3rd order stratigraphic sequences have been recognised. Interpreted sedimentological logs and field photographs are presented in the supplementary data.

Lower Aptian – Sequence 1

The lower part of the Tiskatine section (**MTTK 157 – 161a**) is dominated by wave-influenced shoreface sedimentation overlain by lower shoreface conditions. The interval is barren in foraminifera and calcareous nannofossil but yields abundant ammonoids. Between **MTTK 159** to **160b** lack in mesopelagic phylloceratids and lytoceratids, and the abundance of the shallow nekton-

643 benthic douvilleiceratid *Procheloniceras* (Westermann, 1990, 1996) suggest a distal neritic setting
644 (Frau et al., 2017a).
645 A 3rd order **sequence boundary** around the lower/upper Aptian boundary is recognized between
646 **MTTK 160b** and **161a**, well constrained by ammonoid biostratigraphy (Luber et al. 2017).
647
648 **Upper Aptian – Sequence 2**
649 A subsequent initial transgressive surface (**ITS**) and condensation are recognised in **MTTK 161a**.
650 Here the occurrence of phylloceratids and desmoceratids indicates a brief episode of open-marine
651 conditions at the top of the Bouzergoun Fm.; albeit the fauna is still largely dominated by nekton-
652 benthic forms such as *Epicheloniceras*. The rich and diverse mix of epipelagic and mesopelagic
653 assemblages form a typical Type 2 Horizon of Faunal Uniformity (HUF) and is interpreted to be the
654 result of sea level rise and flooding events (Bulot, 1993).
655 In **MTTK 162** a rapid increase in water depth and the establishment of shelfal conditions is
656 indicated by first occurrence planktonic nannoflora and an increase in foraminifera and calcareous
657 nannofossil recovery. A lithological disconformity from sandstones to marls and increased carbonate
658 content is also recognised between **MTTK 162 and 163.**
659 The establishment of shelfal conditions at Id Amran predates (*P. dechauxi* Zone) the
660 establishment at Tiskatine (*C. tobleri* Zone), while at Assaka this time interval is marked as erosive
661 surfaces.
662 The increase in base-level recognized in **MTTK 162** can be observed regionally and is
663 interpreted as a 3rd order **transgressive systems tract** (**TST**) starting with **MTTK 161a**.
664 Between **MTTK 164** – **MTTK 232** the proportion of planktonic foraminifera seldom falls below 50
665 %, indicating water depths of 50 – 200 m (Murray, 1991) suggesting middle to outer shelf conditions.
666 High relative abundance (65% - 81%) of planktonic foraminifera (notably *Hedbergella* spp.), a
667 prominent increase in abundance and diversity of calcareous nannofossil from **MTTK 162** through to
668 **MTTK 165b,** and higher carbonate content suggest good open-marine conditions. Therefore, **MTTK**

669 **164/165** ("*E.*" *marocanus* Subzone) is interpreted as a **lower upper Aptian maximum flooding**
670 **surface (MFS)**. Regional flooding within the *C. tobleri* Zone is followed by relative continuous
671 deposition in the Tiskatine and Id Amran sections and is also recorded at Assaka (**MTAS 121**).
672 The interval from **MTTK 166 – 191** is interpreted as multiple parasequences in a third order **high**
673 **stand systems tract (HST)**. Sample **MTTK 183b** contains common reworked *Epistomina* derived from
674 shallow shelf environments. The abundance of ammonites decreases significantly and fauna is
675 dominated by the endemic "*E.*" *marocanus*. The same is true at Id Amran between **MTIA 109** to **130.**
676 Between **MTTK 184** to **194**, and even up to **MTTK 203** the ammonite fauna is characterised by
677 the abundance of the cosmopolitan *A. aschiltaensis* and *P.* gr. *ramososeptatum* indicating restored
678 open-marine connections between the EAB and the Mediterranean-Caucasian Tethys. This is also
679 recognised at Id Amran (**MTIA 131** to **142**) and elements are further recorded in Assaka (**MTAS 123**).
680 **MTTK 192** stands out in the field characterised by an erosive base, interpreted as a 3rd order
681 **sequence boundary**. **MTTK 192** has higher siliciclastic content and is barren of foraminifera, but
682 yields large ammonoids (*Pseudoaustraliceras*).
683 The lower Aptian succession is expanded at Id Amran compared to Tiskatine.This changes above
684 the regional flooding in the *C. tobleri* Zone and the upper Aptian succession is compressed in Id
685 Amran compared to Tiskatine and the Id Amran section records a higher siliciclastic input.
686
687 **Upper Aptian – Sequence 3**
688 The top of **MTTK 194** is interpreted as the **ITS.** A rich and diverse ammonite assemblage
689 between **MTTK 206** – **MTTK 213** and increased recovery of foraminifera and calcareous nannofossils
690 between **MTTK 211** – **MTTK 215** suggest the presence of an **upper Aptian MFS** between **MTTK 206** –
691 **MTTK 215** (*E. tiskatinensis* Subzone) with Horizons of Faunal Uniformity. This brackets a 3rd order
692 transgressive systems tract (**TST**) between top **MTTK 194** and **MTTK 215**, which is also recognised at
693 **Id Amran** (**MTIA 149 – 150 top**). At Assaka elements of the *E. tiskatinensis* Subzone are also recorded
694 in poly-phased horizons and polyzonal lenses (**MTAS 123**) infilling erosional surfaces.

695 Overall the upper part of the Tamzergout Fm. at Tiskatine, particularly **MTTK 206** to **231**, is
696 marked by the high abundance and diversity of small-sized epipelagic forms (*Elsaisabellia*,
697 *Protacanthoplites* and "*Hypacanthoplites*") combined with spot occurrences of mesopelagic
698 desmoceratids, indicating the restoration of fully open-marine condition.
699 The interval **MTTK 216 to MTTK 247** is overall still rich in foraminifera, but the interval from
700 **MTTK 232** to **247** is barren in ammonoids and a continuous decline of planktonic foraminifera (50%
701 to <30%) is noted from **MTTK 233** upward. Further, reworking of shelfal *Epistomina* is particularly
702 evident in **MTTK 223** – **MTTK 237**. Calcareous nannofossils are still abundant in this interval, with
703 **MTTK 239** yielding the richest nannoflora of the whole section. Therefore, **MTTK 216** – **MTTK 247** is
704 interpreted as a **HST.** This interval is absent at Id Amran.
705 Clastic progradation is heralded by a marked reduction in diversity and abundance of calcareous
706 nannofossils in bed **MTTK 247. MTTK 247** further shows a noteworthy increase in abundance of
707 reworked *Epistomina* (the highest numbers recorded in any sample). Obviously transported
708 specimens may be indicative of episodes of shelf erosion and redeposition. It is uncertain if these are
709 the results of autocyclic processes affecting the shelf (e.g. severe storms) or of allocyclic processes
710 such as lowering of relative sea-level.Increase in abundance of *Epistomina* and diversity decrease of
711 calcareous nannofossils may indicate of the onset of a shallowing event which ultimately led to the
712 development of a **sequence boundary** at the base of **MTTK 248** identified at Tiskatine. This sequence
713 boundary is more notably expressed at Id Amran (base **MTIA 154**) and DSDP boreholes 370 and 416.
714 At DSDP 370 all the lower and upper Aptian succession exposed at Tiskatine is eroded and only older
715 lower Aptian strata is preserved (NC6B). Boreholes 370/416 are located to the north of the
716 Essaouira-Agadir Basin in the offshore part of the Doukalla Basin and, therefore, not necessarily
717 directly tied to the evolution of the EAB. Nonetheless, the prominently and apparently regionally-
718 developed uppermost Aptian to Lower Albian sequence boundary is noteworthy. This boundary
719 possibly combines a 3rd and 2nd order sequence boundary. It is well constrained by ammonoids,
720 foraminifera and calcareous nannofossils to occur between the "*Hypacanthoplites* spp." Subzone

and the *M. chihaouiae* Zone and is, therefore, suspected as being close to the Aptian/Albian boundary. Relating this sequence boundary to published eustatic sea-level curves is challenging, but it is here tentatively linked to KAp 7 *sensu* Haq (2014).

A sample from bed **MTTK 249** exhibits a dramatic change in palaeoenvironmental conditions compared to the underlying Aptian deposits. Neritic dominated holococcoliths and nannoconids are rarely recorded whilst a cold-water incursion of *R. parvidentatum* is recorded. A regional palaeo-oceanographic change reflected in the nannofossil assemblage appears to have occurred at the Aptian/Albian boundary.

5.3.2 Palaeogeographic interpretation

Early Aptian

A transect from Id Amran to Assaka (Fig. 16) shows a thinning succession, interpreted to be controlled by reducing accommodation toward the crest of a submerged fault block. During the early Aptian, the following incremental tectonic movement phases can be dated by ammonoid biostratigraphic data along this transect:

(1) *P. dechauxi* – lower *D. forbesi* zones: Constrained by erosion of *P. dechauxi* – *C. tobleri* zones time-equivalent deposits in the distal Assaka section (erosional surface base **MTAS 121**). These zones are present in Tiskatine (**MTTK 159** – **160b**) and Id Amran (**MTIA 86** – **MTIA 98**). In Id Amran preservation of the *D. forbesi* Zone time-equivalent deposits (**MTIA 98**) further constrains the timing of first movement phase.

(2) Lower *D. forbesi* – *D. furcata* zones: Constrained by absence of the upper *D. forbesi* plus the entire *D. deshayesi* zones (= OAE 1a-related time culmination) in Id Amran. *D. forbesi* and *D. furcata* zone age deposits are not recorded in Tiskatine and Assaka and form part of a composite surface including multiple unconformities (hiatus **MTTK 160b – MTTK 161a** and again erosional surface base **MTAS 121**).

747 (3) *D. furcata – C. tobleri* zones: Unconformity constrained by absence of the upper *D. furcata*
748 Zone in Id Amran

749 Lower Aptian tectonic movement phases (1) to (3) are expressed in the sedimentary record as
750 disconformities, generally as surfaces of non-deposition. In the Assaka section, they are combined
751 into the basal erosional surface of **MTAS 121**.

752

753 **Late Aptian**

754 While the early Aptian was marked by increased accommodation and early establishment of
755 shelfal conditions in the Id Amran area, this changes in the late Aptian. The compressed upper
756 Aptian succession compared to Tiskatine is interpreted as a gradual infill of accommodation and
757 onlap towards the crest of the submerged fault block to the west. The absence of the
758 "*Hypacanthoplites"* spp. Subzone at Id Amran is linked to stronger erosion than in Tiskatine at the
759 uppermost Aptian to basal Albian sequence boundary.

760 Towards the crest of the fault block in Assaka the upper Aptian is recorded as a set of horizons
761 marked by poly-phased erosion and sedimentation (**MTAS 122** and **123**). Preserved ammonoid
762 specimens mainly coincide with late Aptian - earliest Albian flooding events in the basin suggesting
763 continuous reworking on the crest of a submerged fault block. It is noteworthy that among the
764 ammonoid assemblage in lenses of **MTAS 123** open-marine fauna (*Hypophylloceras*, *Eotetragonites*
765 and *Ephamulina*) are well-represented. This suggests the crest of the submerged fault block was
766 located on the outer shelf, below storm wave base, open to the ocean in the west and that lenses
767 (**MTAS 123**) formed through winnowing by wave-action and mixing of faunal elements. The N-S
768 orientated crest was located in proximity of the modern coastline.

769 **FIGURE 16: PREFERED PLACEMENT**

770

771 ## 6. Conclusions

772 This paper presents combined high-resolution litho-, bio-, chemo- and sequence

773 stratigraphic data analysis for the Aptian of the NW African Atlantic margin. A reference section is
774 proposed at Tiskatine, offering the most complete outcropping section encountered in the EAB. The
775 results provide new information on ranges of foraminifera and calcareous nannofossils, which
776 importantly have been correlated with the local ammonoid zonation scheme defined for the EAB by
777 Luber et al. (2017). Their wider correlation against type localities and species (e.g. SMAS) is
778 discussed. This study also extends the growing global body of $\delta^{13}C$ data against a high-resolution,
779 biostratigraphically constrained section.

780 Based on the distribution of foraminifera in the Tiskatine section, three widely used upper
781 Aptian zones have been recognized: *G. ferreolensis* Zone*, G. algerianus* Zone, and *H. trocoidea – P.*
782 *bejaouensis* zones. In addition, two standard calcareous nannofossil zones are recognised at
783 Tiskatine: NC7A and NC8A. The calibration of these zones against the SMAS and hence standard
784 chronostratigraphy, implies crucial revisions to previously reported ranges.

785 The $\delta^{13}C_{org}$ curve, as well as the $\delta^{13}C_{carb}$ curve, support the biostratigraphic analysis at Tiskatine
786 and can be correlated with the established curves of the Vocontian and South Provence Basin in SE
787 France. The $\delta^{13}C$ analysis highlights the absence of the OAE 1a equivalent time interval and the
788 uppermost Aptian interval, as indicated by biostratigraphic data.

789 Foraminifera, calcareous nannofossil, and carbon isotope data support the presence of a
790 regional hiatus at the Aptian/Albian boundary in the EAB. Revised age dating using calcareous
791 nannofossils at DSDP boreholes 370 and 416 further indicates the presence of this hiatus associated
792 with a regional unconformity offshore.

793 Based on the integration of biostratigraphic data and sedimentological observations, local
794 tectonics can be discerned during the Aptian along the Atlantic Margin.

795 The robust chronostratigraphic framework presented is a contribution towards regional and
796 super-regional correlations that will aid future palaeo(bio)geographic interpretations.

Acknowledgements

This study forms part of the lead authors PhD at the University of Manchester with the North Africa Research Group (NARG). The authors would like to thank the sponsoring companies of NARG and L'Office National des Hydrocarbures et des Mines (ONHYM) for their continued logistical and scientific support. The constructive comments of the editor in-chief, two anonymous reviewers, and Dr. Christian Linnert (Ruhr-Universität, Bochum) are highly appreciated and improved the manuscript greatly. We thank David Gelsthorpe and the team of the Manchester Museum for curation of all the figured material of this publication. Dr Colin Harris (Hydrocarbons International) is thanked for his role in assisting with the foraminiferal analysis. The Natural History Museum is thanked for allowing access to their SEM facility. Prof. Paul Bown at University College London is thanked for access to nannofossil photographic equipment. Prof. Jens O. Herrle (Goethe-Universität, Frankfurt) and Prof. Wolfgang Kuhnt (Christian-Albrechts-Universität, Kiel) are thanked for providing us with their original δ13C data for Vocontian and South Provence basins. Dr. Gérard Friès (Areva, Astana, Kazhakstan) is thanked for his invaluable support during the revision of the French standard successions. We would further like to acknowledge all field assistants and their invaluable help and input.

References

Aguado, R., Castro, J.M., de Gea, G.A., 1999. Aptian bio-events – an integrated biostratigraphic analysis of the Almadich Formation, Inner Prebetic Domain, SE Spain. Cretaceous Research 20, 663–683.

Allan, J.R., Matthews, R.K., 1982. Isotope signatures associated with early meteoric diagenesis. Sedimentology, 29, 797–817.

Ambroggi, R., 1963. Etude géologique du versant méridional du Haut-Atlas occidental et de la plaine du Souss. Notes et Mémoires du Service Géologique du Maroc 157, 1–322.

Ando, A., Huber, B.T., Premoli Silva, I., 2013. *Paraticinella rohri* (Bolli, 1959) as the valid name for the latest Aptian zonal marker species of planktonic foraminifera traditionally called *bejaouaensis* or *eubejaouaensis*. Cretaceous Research 45, 275–287.

Armstrong, H.A., Brasier, M.D., 2005. Microfossils. Blackwell Publishing Ltd (Wiley-Blackwell), Oxford, 296pp.

Bartenstein, H., Bettenstaedt, F., 1962. Marine Unterkreide (Boreal and Tethys). In: Simon, W., Bartenstein, H., Eds., Leitfossilen der Mikropaläontologie. Berlin: Gebrüder Borntraeger, 225–298.

Baudin, F., Moullade, M., Tronchetti, G., 2008. Characterisation of the organic matter of upper Bedoulian and lower Gargasian strata in the historical stratotypes (Apt and Cassis-la-Bédoule areas, SE France). Carnets de Géologie / Notebooks on Geology 01, 1-9.

841 Behrens, M., Krumsiek, K., Meyer, D.E., Schäfer, A., Siehl, A., Stets, J., Thein, J., Wurster, P., 1978.
842 Sedimentationsabläufe im Atlas-Golf (Kreide Küstenbecken Marokko). Geologische Rundschau 67,
843 424–453.
844
845 Bellier, J.P., Moullade, M., 2002. Lower Cretaceous planktonic foraminiferal biostratigraphy of the
846 western North Atlantic (ODP Leg 171B), and taxonomic clarification of key index species. Revue de
847 Micropaléontologie 45, 9–26.
848
849 Bergen, J.A, 2000. Calcareous Nannofossils from the Lower Aptian Historical Stratotype at Cassis-La
850 Bédoule (SE France). In: Moullade, M., Tronchetti, G., Masse, J.-P., Eds., Le stratotype historique de
851 l'Aptien inférieur (Bédoulien) dans la région de Cassis-La Bédoule (S.E. France), Géologie
852 méditerranéenne 25/3-4 (1998), 227–255.
853
854 Bodin, S., Godet, A., Westermann, S., Föllmi, K. B., 2013. Secular change in northwestern Tethyan
855 water-mass oxygenation during the late Hauterivian-early Aptian. Earth and Planetary Science Letters
856 374, 121–131.
857
858 Bodin, S., Meissner, P., Janssen, N.M.M., Steuber, T., Mutterlose, J., 2015. Large igneous provinces
859 and organic carbon burial: Controls on global temperature and continental weathering during the
860 Early Cretaceous. Global and Planetary Change 133, 238–253.
861
862 Bodin, S., Hönig, M.R., Krencker, F.-N., Danisch, J. and Kabiri, L., 2017. Neritic carbonate crisis during
863 the Early Bajocian: Divergent responses to a global environmental perturbation. Palaeogeography,
864 Palaeoclimatology, Palaeoecology, 468, 184–199.
865

BouDagher-Fadel, M. K., Banner, F.T., Whittaker, J.E., with a contribution from M. D. Simmons, 1997. The Early Evolutionary History of Plank tonic Foraminifera. British Micropalaeontological Society Public Series. Chapman and Hall, London, 269 pp.

Bown, P., Rutledge, D., Crux, J.A., Gallagher, L.T., 1998. Lower Cretaceous. In: Bown, P., Ed., Calcareous Nannofossil Biostratigraphy, 86-131, Chapman and Hall; Kluwer Academic.

Bown, P.R., Young, J.R., 1998. Techniques. In: Bown, Ed., Calcareous Nannofossil Biostratigraphy, 16-28.

Bralower, T.J., Sliter, W.V., Arthur, M.A., Leckie, M.R., Allard, D., Schlanger, S.O., 1993. Dysoxic/Anoxic Episodes in the Aptian-Albian (Early Cretaceous). In: Pringle, M.S., Sager, W.S., Sliter, W.V., Stein, S., Eds, The Mesozoic Pacific. Geology, Tectonics and Volcanism. Geophysical Monograph Series 77, 5–37.

Bulot, L.G., 1993. Stratigraphical implications of the relationship between ammonites and facies; examples from the Lower Cretaceous (Valanginian–Hauterivian) of the Western Tethys: In: House, M.R., Ed., The Ammonoidea: Environment, Ecology and Evolutionary Change, The Systematics Association Special Volume 47, 243–265.

Bulot, L.G., 2010. Appendix. Systematic palaeontology of Aptian and Albian ammonites from southwest Iran. In: Vincent, B., van Buchem, F.S.P., Bulot, L.G., Immenhauser, A., Caron, M., Baghbani, D., Huc A.Y., Carbon–isotope stratigraphy, biostratigraphy and organic matter distribution in the Aptian-Lower Albian successions of southwest Iran (Dariyan and Kazhdumi formations). GeoArabia Special Publication 4/1, 167–195.

892 Bulot, L.G, Latil, J.-L., Hairabian, A., Fournillon, A., 2014. New insight on the genus *Nolaniceras* Casey,
893 1961 (Ammonoidea, Cretaceous) and its consequences on the biostratigraphy of the Aptian Stage.
894 Proceedings of the Geologists' Association 125, 227–232.
895
896 Butt, A., 1982. Micropaleontological bathymetry of the Cretaceous of western Morocco.
897 Palaeogeography, Palaeoclimatology, Palaeoecology 37, 235–275.
898
899 Caron, M., 1985. Cretaceous planktonic foraminifera. In: Bolli, H.M., Saunders, J.B. and Perch-Nielsen,
900 K., Eds., Plankton Stratigraphy, Cambridge University Press, 17-86.
901
902 Damotte, R., Magniez-Jannin, F. 1973. Ostracodes et foraminifères de l'Aptien inférieur du Sondage
903 du Bois du Perchois (Aube). Bulletin d' Information des Géologues du Bassin de Paris 36, 3–47.
904
905 De Gea, G.A., Castro, J.M., Aguado, R., Ruiz-Ortiz, P.A., Company, M., 2003. Lower Aptian carbon
906 isotope stratigraphy from a distal carbonate shelf setting: the Cau section, Prebetic zone, SE Spain.
907 Palaeogeography, Palaeoclimatology, Palaeoecology 200, 207–219.
908
909 Dauphin, L., 2002. Litho-, bio-, et chronostratigraphie comparées dans le Bassin vocontien à l'Aptien.-
910 Unpublished PhD Thesis Université de Lille 1, 451 pp.
911
912 Duffaud, F., Brun, L., Planchut, B., 1966. Le bassin du Sud-Ouest marocain. In: Reyre, D., Ed., Bassins
913 sédimentaires du Littoral africain. Symposium de l'Association des Services géologiques africains
914 (New Dehli, 1964). 1ère partie, Littoral Atlantique, 5–12. Firmin Didot Publications, Paris.
915

916 Dutour, Y., 2005. Biostratigraphie, évolution et renouvellements des ammonites de l'Aptien supérieur
917 (Gargasien) du bassin vocontien (Sud–Est de la France). Unpublished PhD Thesis Lyon 1, 302 pp.
918
919 Ettachfini, M., Company, M., Jaques, R., Taj-Eddine, K., Tavera, J.M., 1998. Le Valanginien du bassin de
920 Safi (Maroc atlantique) et sa faune d'ammonites. Implications paléobiogéographiques. Comptes
921 Rendus de l'Académie des Sciences de Paris, Sciences de la Terre et des Planètes 327, 319–325.
922
923 Föllmi, K.B., Godet, A., Bodin, S., Linder, P., 2006. Interactions between environmental change and
924 shallow-water carbonate build-up along the northern Tethyan margin and their impact on the early
925 Cretaceous carbon-isotope record. Paleoceanography 21, PA4211, 1–16.
926
927 Frau, C., Delanoy, G., Hourquieg, E., 2015. Le genre *Macroscaphites* Meek, 1876 (Ammonoidea) dans
928 l'Aptien inférieur de Cassis-La Bédoule (Bouches-du-Rhône, France). Proposition d'un nouveau
929 schéma zonal pour la série stratotypique. Revue de Paléobiologie 34, 45–57.
930
931 Frau C., Delanoy G., Masse J.-P., Lanteaume C., Tendil, A.J.B., 2016. New Heteroceratidae
932 (Ammonoidea) from the late Barremian deepening succession of Marseille (Bouches–du–Rhône,
933 France). Acta Geologica Polonica 66/2, 179–199.
934
935 Frau C., Pictet, A., Spangenberg, J., Masse J.-P., Tendil, A.J.B., Lanteaume C., 2017a. New insights on
936 the age of the post-Urgonian marly cover of the Apt region (Vaucluse, SE France) and its implications
937 on the demise of the North Provence carbonate platform. Sedimentary Geology, in press.
938
939 Frau, C., Bulot, L.G., Delanoy, G., Moreno-Bedmar, J.A., Masse, J.-P., Tendil, A.J.-B., Lanteaume, C.,
940 2018. The candidate Aptian GSSP at Gorgo a Cerbara (Central Italy): an alternative interpretation of
941 the bio-, litho- and chemostratigraphic markers. Newsletter on Stratigraphy 51, 311-326

Godet, A., Hfaiedh, R., Arnaud-Vanneau, A., Zghal, I., Arnaud, H., Ouali, J., 2014. Aptian palaeoclimates and identification of an OAE1a equivalent in shallow marine environments of the southern Tethyan margin: Evidence from Southern Tunisia (Bir Oum Ali section, Northern Chott Chain). Cretaceous Research 48, 110–129.

Haq, B., 2014. Cretaceous eustasy revisited. Global and Planetary Change 113, 44–58.

Herrle, J.O., Mutterlose, J., 2003. Calcareous nannofossils from the Aptian–Lower Albian of southeast France: palaeoecological and biostratigraphic implications. Cretaceous Research 24, 1-22.

Herrle, J.O., Kössler, P., Friedrich, O., Erlenkeuser, H., Hemleben, C., 2004. High-resolution carbon isotope records of the Aptian to Lower Albian from SE France and the Mazagan Plateau (DSDP Site 545): a stratigraphic tool for paleoceanographic and paleobiologic reconstruction. Earth and Planetary Science Letters 218, 149–161.

Immenhauser, A., Kenter, J.A.M., Ganssen, G., Bahamonde, J.R., Van Vliet, A., Saher, M.H., 2002. Origin and Significance of Isotope Shifts in Pennsylvanian Carbonates (Asturias, NW Spain). Journal of Sedimentary Research 72, 82–94.

Jeremiah, J., 1996. A proposed Albian to lower Cenomanian nannofossil biozonation for England and the North Sea basin. Journal of Micropalaeontology 15, 97– 129.

Jeremiah, J., 2000. Lower Cretaceous turbidites of the Moray Firth: sequence stratigraphical framework and reservoir distribution. Petroleum Geoscience 6, 309-328, Supplementary Publication No. SUP 18155, 1-19.

Jeremiah, J., 2001. A Lower Cretaceous nannofossil zonation for the North Sea Basin. Journal of Micropalaeontology 20, 45–80.

Jeremiah, J.M., Duxbury, S., Rawson, P., 2010. Lower Cretaceous of the southern North Sea Basins: reservoir distribution within a sequence stratigraphic framework. Netherlands Journal of Geosciences / Geologie en Mijnbouw 89, 203–237.

Kennedy, W.J., Gale, A.S., Bown, P.R., Caron, M., Davey, R.J., Gröcke, D., Wray, D.S., 2000. Integrated stratigraphy across the Aptian-Albian boundary in the Marnes Bleues, at the Col Pré-Guittard, Arnayon (Drôme), and at Tartonne (Alpes-de-Haute-Provence), France: a candidate Global Boundary Stratotype Section and Boundary Point for the base of the Albian Stage. Cretaceous Research 21, 591–720.

Kennedy, W.J., Gale, A.S., Huber, B.T., Petrizzo, M.R., Bown, P., Barchetta, A., Jenkyns, H.C., 2014. Integrated stratigraphy across the Aptian/Albian boundary at Col de Pré-Guittard (southeast France): A candidate Global Boundary Stratotype Section. Cretaceous Research 51, 248–259.

Kilian, W., Gentil, L., 1906. Découverte de deux horizons crétacés remarquables au Maroc. Comptes rendus sommaire de l'Académie des Sciences de Paris 142, 603–605.

Kuhnt, W., Moullade, M., 2007. The Gargasian (Middle Aptian) of La Marcouline section at Cassis-La Bédoule (SE France): Stable isotope record and orbital cyclicity. Carnets de Geologie, Article 2007/02, 9 p.

993 Kuhnt, W., Holbourn, A., Moullade, M., 2011. Transient global cooling at the onset of early Aptian
994 oceanic anoxic event (OAE) 1a. Geology 39: 323–326.
995
996 Latil, J.-L., 2011. Early Albian ammonites from Central Tunisia and adjacent areas of Algeria. Revue
997 de Paléobiologie 30/1, 321–429.
998
999 Laville, E., Pique, A., Amrhar, M., Charroud, M., 2004. A restatement of the Mesosoic Atlasic Rifting
1000 (Morocco). Journal of African Earth Sciences 38, 145–153.
1001
1002 Lehmann, J., Friedrich, O., von Bargen, D., Hemker, T., 2012. Early Aptian bay deposits at the southern
1003 margin of the lower Saxony Basin: Integrated stratigraphy, palaeoenvironment and OAE 1a. Acta
1004 Geologica Polonica 62/1, 35–62.
1005
1006 Lehmann, J., von Bargen, D., Engelke, J., Claßen, J., 2016: Morphological variability
1007 in response to palaeoenvironmental change – a case study on Cretaceous ammonites.
1008 Lethaia 49, 73–86.
1009
1010 Luber, T.L., Bulot, L.G., Redfern, J., Frau, C., Arantegui, A., Masrour, M., 2017. A revised ammonoid
1011 biostratigraphy for the Aptian of NW Africa: Essaouira-Agadir Basin, Morocco. Cretaceous Research
1012 79, 12–34.
1013
1014 Marshall, J.D., 1992. Climatic and oceanographic isotopic signals from the carbonate rock record and
1015 their preservation. Geological Magazine, 129(2): 143–160.
1016

1017 McAnena, A., Flögel, S., Hofmann, P., Herrle, J. O., Griesand, A., Pross, J., Talbot, H. M., Rethemeyer,
1018 J., Wallmann, K., and Wagner, T., 2013. Atlantic cooling associated with a marine biotic crisis during
1019 the mid-Cretaceous period. Nature Geoscience, 6: 558–561.
1020
1021 Menegatti, A.P., Weissert, H., Brown, R.S., Tyson, R.V., Farrimond, P., Strasser, A. and Caron, M., 1998.
1022 High-resolution $\delta^{13}C$ stratigraphy through the early Aptian "Livello Selli" of the Alpine Tethys.
1023 Paleoceanography 13, 530–545.
1024
1025 Meyer, D., 1978. Microfacies and microfabrics of Early Middle Cretaceous sediments selected from
1026 site 370, DSDP Leg 41 (deep basin off Morocco). In: Gardner, J. and Herring, J., Eds., Initial reports of
1027 the deep sea drilling project 41, 961–981.
1028
1029 Moullade, M., 1966. Étude stratigraphique et micropaléontologique du crétacé inférieur de la "fosse
1030 vocontienne". Documents des Laboratoires de Géologie de la Faculté des Sciences de Lyon 15, 1–
1031 369.
1032
1033 Moullade, M., Tronchetti, G., Busnardo, R., Masse, J.-P., 2000. Description lithologique des coupes
1034 types du stratotype historique de l'Aptien inférieur dans la région de Cassis-La Bédoule (SE France).
1035 In: Moullade, M., Tronchetti, G., Masse, J.-P., Eds., Le stratotype historique de l'Aptien inférieur
1036 (Bédoulien) dans la région de Cassis-La Bédoule (S.E. France), Géologie méditerranéenne 25/3-4
1037 (1998), 15–29.
1038
1039 Moullade, M., Bellier, J.P., Tronchetti, G., 2002. Hierarchy of criteria, evolutionary processes and
1040 taxonomic simplification in the classification of Lower Cretaceous planktonic foraminifera.
1041 Cretaceous Research 23, 111–148.
1042

1043 Moullade, M., Tronchetti, G., Bellier, J.P., 2005. The Gargasian (Middle Aptian) strata from Cassis-La
1044 Bédoule (Lower Aptian historical stratotype, SE France): planktonic and benthic foraminiferal
1045 assemblages and biostratigraphy. Carnets de Géologie, Article CG2005_A02.
1046
1047 Murray, J.W., 1991. Ecology and palaeoecology of benthic foraminifera. Wiley, 397 pp.
1048
1049 Nouidar, M., Chellai, H., 2001. Facies and sequence stratigraphy of a Late Barremian wave-
1050 dominated deltaic deposit, Agadir Basin, Morocco. Sedimentary Geology 150, 375-384.
1051
1052 Ogg, J.G., Hinnov, L.A., 2012. Cretaceous. In: Gradstein, F.M, Ogg, J.G., Schmitz, M., Ogg, G., Eds., The
1053 Geologic Time Scale 2012, Elsevier, 793–853.
1054
1055 Owen, H.G., 1996. Boreal and Tethyan late Aptian to late Albian ammonite zonation and
1056 palaeobiogeography. Mitteilungen aus dem Geologisch-Paläontologischen Institut der Universität
1057 Hamburg 77, 461–481.
1058
1059 Perch-Nielsen, K., 1985. Mesozoic calcareous nanofossils. In: Bolli, H.M., Saunders, J.B., Perch-
1060 Nielsen, K., Eds., Plankton Stratigraphy. Cambridge University Press, Cambridge, 329-426.
1061
1062 Peybernes, C., Giraud, F., Jaillard, E., Robert, E., Masrour, M., Aoutem, M., Içame, N., 2013.
1063 Stratigraphic framework and calcareous nannofossil productivity of the Essaouira-Agadir Basin
1064 (Morocco) during the Aptian-Early Albian: Comparison with the north-Tethyan margin. Cretaceous
1065 Research 39, 149–169.
1066
1067 Phelps, M. R., Kerans C., Da-Gama, R.O.B.P., Jeremiah, J., Hull, D, Robert G., Loucks, R.G., 2015.
1068 Response and recovery of the Comanche carbonate platform surrounding multiple Cretaceous

1069 oceanic anoxic events, northern Gulf of Mexico. Cretaceous Research 54, 117–144 (Supplementary
1070 Data).
1071
1072 Premoli Silva, I., Verga, D., 2004. Practical Manual of Cretaceous Planktonic Foraminifera. In: Verga,
1073 D., Rettori, R., Eds., International School on Planktonic Foraminifera, Universities of Perugia and
1074 Milano, Tipografia Pontefelcino, Perugia.
1075
1076 Reboulet, S., Giraud F., Proux O., 2005.Ammonoid abundance variations related to changes in trophic
1077 conditions across the Oceanic Anoxic Event 1d (Latest Albian, SE France). Palaios 20, 121–141.
1078
1079 Reboulet, S., Rawson, P.F., Moreno-Bedmar, J.A. (reporters), Aguirre-Urreta, M.B., Barragán, R.,
1080 Bogomolov, Y., Company, M., González-Arreola, C., Idakieva Stoyanova, V., Lukeneder, A., Matrion, B.,
1081 Mitta, V., Randrianaly, H., Vašíček, Z., Baraboshkin, E.J., Bert, D., Bersac, S., Bogdanova, T.N., Bulot,
1082 L.G., Latil, J.-L., Mikhailova, I.A., Ropolo, P., Szives, O., 2011. Report on the 4th International Meeting
1083 of the IUGS Lower Cretaceous Ammonite Working Group, the “Kilian Group” (Dijon, France, 30th
1084 August 2010). Cretaceous Research 32, 786–793.
1085
1086 Reboulet, S., Szives, O., Aguirre-Urreta, B., Barragán, R., Company, M., Idakieva, V., Ivanov, M.,
1087 Kakabadze, M.V., Moreno-Bedmar, J.A., Sandoval, J., Baraboshkin, E.J., Çağlar, M.K., Főzy, I., González-
1088 Arreola, C., Kenjo, S., Lukeneder, A., Raisossadat, S.N., Rawson, P.F., Tavera, J.M., 2014. Report on the
1089 5th International Meeting of the IUGS Lower Cretaceous Ammonite Working Group, the Kilian Group
1090 (Ankara, Turkey, 31st August 2013). Cretaceous Research 50, 126–137.
1091
1092 Rey, J., Canérot, B., Peybernès, B., Taj-Eddine, K., Rahhali, I., Thieuloy, J.-P., 1986. Le Crétacé inférieur
1093 de la région d'Essaouira: données biostratigraphiques et évolutions sédimentaires. Revue de la

1094 Faculté des Sciences de Marrakech, Numéro spécial 2, 413–411.

1095

1096 Rey, J., Canérot, J., Peybernès, B., Taj-Eddine, K., Thieuloy, J.-P., 1988. Lithostratigraphy,
1097 biostratigraphy and sedimentary dynamics of the Lower Cretaceous deposits on the northern side of
1098 the western High Atlas (Morocco). Cretaceous Research 9, 141–158.

1099

1100 Robaszynski, F., Caron, M., 1995. Foraminiferes planctoniques du Crétacé: commentaire de la
1101 zonation Europe-Méditerranée. Bulletin de la Société Géologique de France 166, 681–692.

1102

1103 Roch, E., 1930. Etudes géologiques dans la région méridionale du Maroc Occidental. Notes et
1104 Mémoires du Service des Mines et de la Cartes Géologiques Maroc 9, 1–542.

1105

1106 Roth, P. H., 1978. Cretaceous nannoplankton biostratigraphy and oceanography of the northwestern
1107 Atlantic Ocean: Initial Reports of the Deep-Sea Drilling Project 44, 731–759.

1108

1109 Roth, P. H., 1983. Jurassic and Lower Cretaceous calcareous nannoplankton in the western North
1110 Atlantic (Site534): biostratigraphy, preservation and some observations on biogeography and
1111 palaeoceanography. In: Winterer, E.L., Ewing, J.I., Eds., Initial Reports of the Deep Sea Drilling
1112 Projects, 76, 587-621.

1113

1114 Sigal, J., 1977. Essai de zonation du Crétacé du Méditerrannéen a l'aide des foraminiféres
1115 planctoniques. Géologie Méditerranéenne 4, 99–108.

1116

1117 Street, C., Bown., P.R., 2000. Palaeobiogeography of Early Cretaceous (Berriasian-Barremian)
1118 calcareous nannoplankton. Marine Micropaleontology 39, 265–291.

1119

1120 Tari, G., Jabour, H., 2013. Salt tectonics along the Atlantic margin of Morocco. Geological Society,
1121 London, Special Publications 369, 337–353.

1122

1123 Tremolada, F., Erba, E., 2002. Morphometric analysis of the Aptian *Rucinolithus terebrodentarius* and
1124 *Assipetra infracretacea* nannoliths: implications for taxonomy, biostratigraphy and
1125 paleoceanography. Marine Micropaleontology 44, 77–92.

1126

1127 Verga D., Premoli Silva, I., 2003a. Early Cretaceous planktonic foraminifera from the Tethys: the large,
1128 many–chambered representatives of the genus *Globigerinelloides*. Cretaceous Research 24, 661–690.

1129

1130 Verga D., Premoli Silva, I., 2003b. Early Cretaceous planktonic foraminifera from the Tethys: small
1131 few–chambered representatives of the genus *Globigerinelloides*. Cretaceous Research 24, 305–334

1132

1133 Westermann, G.E.G., 1990. New developments in ecology of Jurassic–Cretaceous Ammonoids. In
1134 Pallini, G., Cecca, F., Cresta, S., Santantonio, M., Eds., Fossili, Evoluzione, Ambiente, Atti del Secondo
1135 Convegno Internazionale, Pergola, 1987, Comite Centenerio Raffaele Piccinini, 459–478.

1136

1137 Westermann, G.E.G., 1996. Ammonoid life and habitat. In Landman, N.H., Tanabe, K., Davis, R.A.,
1138 Eds., Ammonoid Paleobiology, Topics in Geobiology 13, 607-707.

1139

1140 Westermann, G.E.G, 2000. Marine faunal realms of the Mesozoic: review and revision under the new
1141 guidelines for biogeographic classification and nomenclature. Palaeogeography, Palaeoclimatology,
1142 Palaeoecology 163, 49–68.

1143

1144 Witam, O., 1998. Le Barrémien-Aptien de l'Atlas Occidental (Maroc) : lithostratigraphie,
1145 biostratigraphie, sédimentologie, stratigraphie séquentielle, géodynamique et paléontologie. Strata

30, 1–421.

Yamina, B., Ali Nabiha, B. H., Saloua, R., Kamal, T., 2002. Etude biostratigraphique du Crétacé inférieur (Barrémien supérieur- Albien) du Haut Atlas occidental (MAROC). Estudios Geologicos 58, 105–112.

Figure Captions

Figure 1. Overview. **Inset:** Location map of Morocco and position of the DSDP well 370 offshore (reference coordinate system WGS 84). **Main:** Digital elevation model of the Essaouira-Agadir Basin (EAB) with sections studied and sub-crop of the geological map showing Lower Cretaceous outcrops and main anticlines and synclines.

Figure 2. Generalised lithostratigraphy of the upper Barremian to Lower Albian strata in the west-central part of the EAB with broad depositional environments andt key age interpretations.

Figure 3 Tiskatine section. Distribution of samples studied for foraminifera and calcareous nannofossil analysis and field photograph of key section intervals. Distribution charts can be found in the supplementary data. Abbreviations: Ammon. – Ammonite, Bouzerg. – Bouzergoun, grad. – grading, Grav. – Gravel, l. – lower, ITS – Initial Transgressive Surface, O. Tid. – Oued Tidzi, Oy. – Oyster, p.p. – pro parte, Rud. – Rudstone, SB – Sequence Boundary, Tob. – Tobleri, W.st. – Wackestone

Figure 4. Id Amran section. Distribution of ammonoids, key calcareous nannofossils, and biostratigraphic interpretation. Distribution charts for calcareous nannofossil can be found in the supplementary data.

Figure 5. Assaka section. Ammonoid distribution and biostratigraphic interpretation.

Figure 6. DSDP borehole 370: Lithostratigraphic log and calcareous nannofossil distribution. Distribution charts for calcareous nannofossil can be found in the supplementary data.

1178 Figure 7. Distribution of key planktonic foraminifera species and zonation (after Premoli and Verga,
1179 2004) against the local ammonoid zonation scheme in the EAB of Luber et al. (2017) and the
1180 Standard Mediterranean Ammonite Scale (SMAS) of Reboulet et al. (2011, 2014).
1181
1182 Figure 8. Plate 1: Scanning electron microscope images of selected planktonic foraminifera from the
1183 Tiskatine section, Morocco (all scale bars = 0.1mm): (1-3) *Globigerinelloides barri* (Bolli, Loeblich and
1184 Tappan, 1957) from **MTTK 197**; (4-6) *Globigerinelloides ferreolensis* (Bolli, Loeblich and Tappan,
1185 1957) from **MTTK 197**; (7-8) *G. ferreolensis* - *G. algerianus* transitional form from **MTTK 185a**; (9-11)
1186 *Globigerinelloides algerianus* Cushman and Ten Dam, 1948 from **MTTK 197**; (12-13)
1187 *Pseudoplanomalina cheniourensis* (Sigal, 1952) from **MTTK 217**; (14-15) *Pseudoplanomalina*
1188 *cheniourensis* (Sigal, 1952) from **MTTK 237**
1189
1190 Figure 9. Plate 2: Scanning electron microscope images of selected planktonic foraminifera from the
1191 Tiskatine section, Morocco (all scale bars = 0.1mm): (1) ?*Paraticinella bejaouaensis* (Sigal, 1966) from
1192 **MTTK 247**; (2-4) *Hedbergella trocoidea* (Gandolfi, 1942) from **MTTK 235**; (5-6) *Tritaxia dividens*
1193 (Grabert, 1959), smaller morphotype, from **MTTK 227**; (7-8) *Gavelinella* cf. *barremiana* Bettenstaedt,
1194 1952 from **MTTK 221**; (9-11) *Conorotalites aptiensis* (Bettenstaedt, 1952) from **MTTK 219**; (12)
1195 *Lenticulina muensteri* (Roemer, 1839) from **MTTK 215**; (13-15) *Valvulineria gracillima* Ten Dam, 1947
1196 from **MTTK 227**
1197
1198 Figure 10. Calcareous nannofossil photographic plate of key specimen from the Tiskatine and Id
1199 Amran onshore sections and DSDP borehole 370. Scale bar in all photos is 5µm.
1200
1201 Figure 11. Ammonoid photographic plate of the Id Amran section: (1-2) *Deshayesites* aff. *callidiscus*
1202 Casey, 1961a from bed **MTIA 98** ((Manch) LL. 16142); (3-9) *Dufrenoyia praedufrenoyi* Casey, 1964
1203 from bed **MTIA 100** ((Manch) LL. 16144); (10) *Toxoceratoides rochi* Casey, 1961b from bed **MTIA 100**

((Manch) LL. 16145); (11-17) "*Prochelonicera*s" sp. nov. from bed **MTIA 98** ((Manch) LL. 16143)

Figure 12. Ammonoid photographic plate of the Assaka section: (1-2) *Epicheloniceras* gr. *waageni* (Anthula, 1900) – *tschernyschewi* (Sinzow, 1906) from bed **MTAS 122** ((Manch) LL. 16147); (3) *Pseudoaustraliceras* gr. *ramososeptatum* (Anthula, 1900) from bed **MTAS 123** ((Manch) LL. 16149); (4-5) *Epicheloniceras* gr. *gracile* Casey, 1961a from bed **MTAS 121** ((Manch) LL. 16146); (6-7) *Epicheloniceras* gr. *subbuxtorfi* – *paucinodum* (Burckhardt, 1925) from bed **MTAS 122** ((Manch) LL. 16148); (8) "*Hypacanthoplites*" cf. *paucicostatus* (Breistroffer *in* Dubourdieu, 1953) from bed **MTAS 123** ((Manch) LL. 16150); (9-10) *Mellegueiceras* cf. *chihaouiae* Latil, 2011 from bed **MTAS 123** ((Manch) LL. 16151); (11-12) *Pseudoaustraliceras* gr. *ramososeptatum* (Anthula, 1900) from bed **MTAS 123** ((Manch) LL. 16152)

Figure 13. Integrated biostratigraphic chart of the Tiskatine section, EAB. Local ammonoid zonation scheme of Luber et al. (2017), foraminifera zonation after Premoli and Verga (2004) and calcareous nannofossil zonation after Roth (1978) and Bralower et al. (1993). Distribution charts for foraminifera and calcareous nannofossil can be found in the supplementary data.

Figure 14. Carbonate content, total organic carbon (TOC), $\delta^{13} C_{carb}$ and $\delta^{13} C_{org}$ (‰ VDPB) of the lower Aptian to Lower Albian at Tiskatine, EAB. Findings are referenced against the local ammonoid zonation scheme in the EAB of Luber et al. (2017), the Standard Mediterranean Ammonite Scale (SMAS) of Reboulet et al. (2011, 2014), standard planktonic foraminiferal zonation of Premoli and Verga (2004) and Lower Cretaceous NC Zones of Roth (1978, 1983) and subzones after Bralower et al. (1993).

Figure 15. Comparison of lower Aptian to Lower Albian $\delta^{13} C_{carb}$ and $\delta^{13} C_{org}$ (‰ VDPB) at Tiskatine, EAB and $\delta^{13} C_{carb}$ (‰ VDPB) in the Vocontian Basin (data from Herrle, 2004). Two negative shifts of

1230 the succession are highlighted by grey shading bands and diagenetically altered data annotated.
1231 Data is references against the local ammonoid zonation scheme in the EAB of Luber et al. (2017), the
1232 Standard Mediterranean Ammonite Scale (SMAS) of Reboulet et al. (2011, 2014), standard
1233 planktonic foraminiferal zonation of Premoli and Verga (2004) and Lower Cretaceous NC Zones of
1234 Roth (1978, 1983) and subzones after Bralower et al. (1993).
1235
1236 Figure 16. Sequence stratigraphic correlation of the Id Amran, Tiskatine and Assaka section based on
1237 ammonoid biostratigraphy with associated Wheeler Diagram. Data is referenced to the local
1238 ammonoid zonation scheme in the EAB of Luber et al. (2017), the Standard Mediterranean
1239 Ammonite Scale (SMAS) of Reboulet et al. (2011, 2014). Duration of ammonoid zones are derived
1240 from Dauphin, 2002.
1241

Captions Supplementary Data

Supplementary dataset 1: Distribution chart of key foraminifera from the Tiskatine section.

Supplementary dataset 2: Distribution chart of key calcareous nannofossils from the Tiskatine section.

Supplementary dataset 3: Distribution chart of key calcareous nannofossils from the Id Amran section.

Supplementary dataset 4: Distribution chart of key calcareous nannofossils from the DSDP borehole 370 cores section 34/1 – 31/4 and DSDP borehole 416 core 6-4 and 6 CC.

Supplementary dataset 5: Overview of studied sections.

Supplementary dataset 6: Detailed log with depositional environment interpretation and field photographs of the Tiskatine section.

Supplementary dataset 7: Detailed log with depositional environment interpretation and field photographs of the Id Amran section.

Supplementary dataset 8: Detailed log with depositional environment interpretation and field photographs of the Assaka section.

Supplementary dataset 9: Distribution of key ammonoid (Dauphin, 2002; Dutour, 2005; Bulot and Frau, in progress), foraminifera (Kennedy et al., 2000, 2014; Dauphin, 2002) and calcareous

1268 nannofossils (Herrle and Mutterlose, 2003; Kennedy et al., 2000, 2014) of the Vocontian Basin of SE
1269 France.
1270
1271 Supplementary dataset 10: Distribution of key ammonoids (Frau et al., 2015; Frau and Bulot in
1272 progress), foraminifera (Moullade et al., 2000, 2005) and calcareous nannofossils (Bergen, 2000) of
1273 the Marcouline section, South Provence Basin. $\delta^{13}C$ data from Kuhnt et al. (2007) and TOC data from
1274 (Moullade et al., 2000).
1275
1276 Supplementary dataset 11: Distribution of key ammonoid (Frau et al., 2015; Frau and Bulot in
1277 progress), foraminifera (Moullade et al., 2000, 2005) and calcareous nannofossil (Bergen, 2000)
1278 specimen from the Cassis section, South Provence Basin.

10°0'00" W

9°0'00" W

32°0'00" N

31°0'00" N

Essaouira - Agadir Basin

Km
0 250 500
N

DSDP 370

Rabat

Morocco

Marrak.

Essaouira - Agadir Basin

Tan Tan

Dakhla

Essaouira

ATLANTIC OCEAN

Chichaoua escarpment

Tidzi Diapir

Jbel Amsittene

Imi'n'Tanout

Tamanar

Tiskatine

Assaka

Id Amran

Argana Valley

Cap Ghir

Souss Plain

Agadir

Km
0 25 50

Major Anti/Synclines

Lower Cretaceous Outcrops

10°0'00" W

9°0'00" W

31°0'00" N

Rey et al., 1988	upper Barremian	lower Aptian	u. Apt. ..... Albian
Nouidar and Chellai, 2001	upper Barremian / l. Apt.	mid. Aptian	(not sudied)
This Study	u. Barremian ..... ? ..... lower Aptian	upper Aptian	Lower Albian
	Bouzergoun Fm.	Tamzergout Fm.	Oued Tidzi Fm.

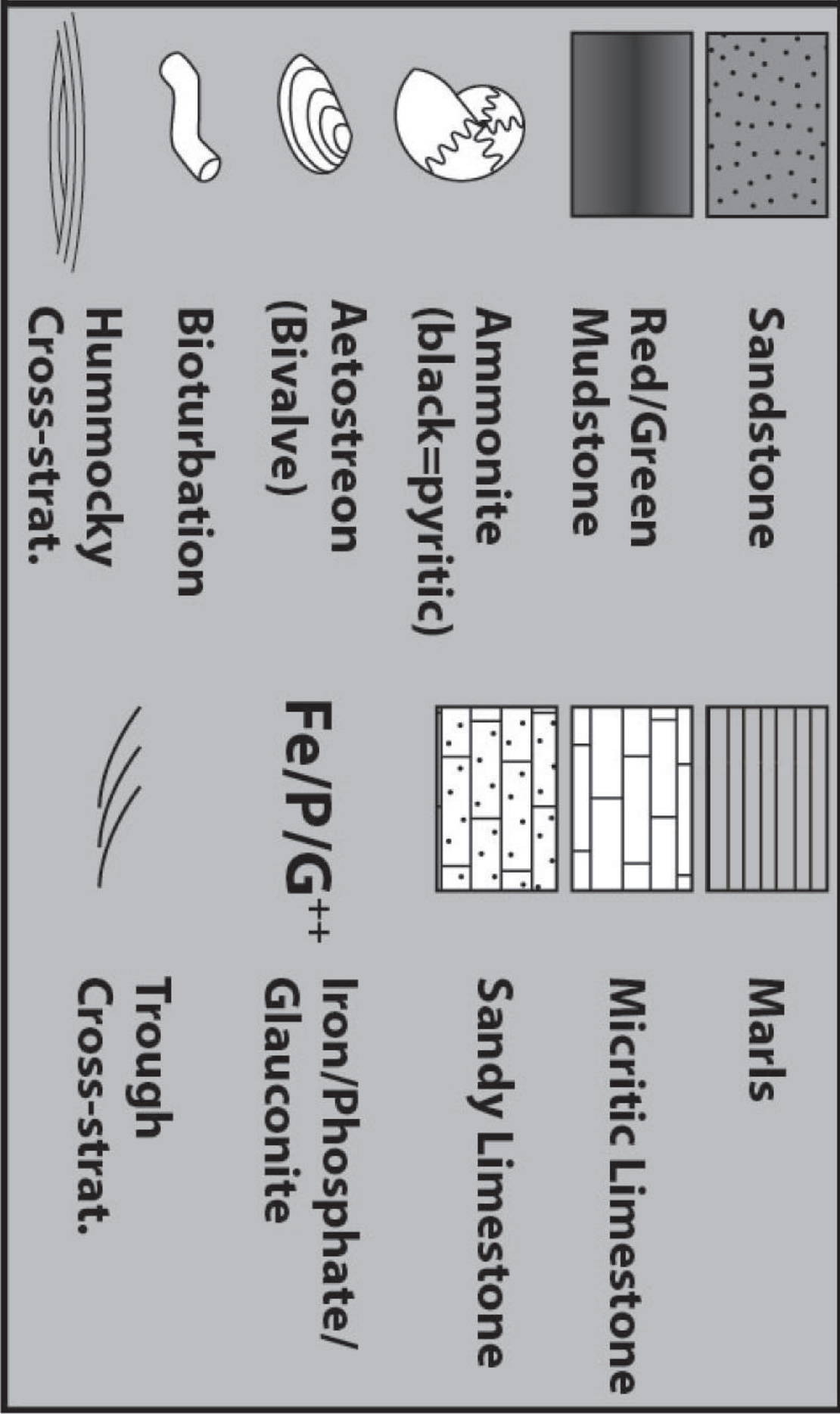

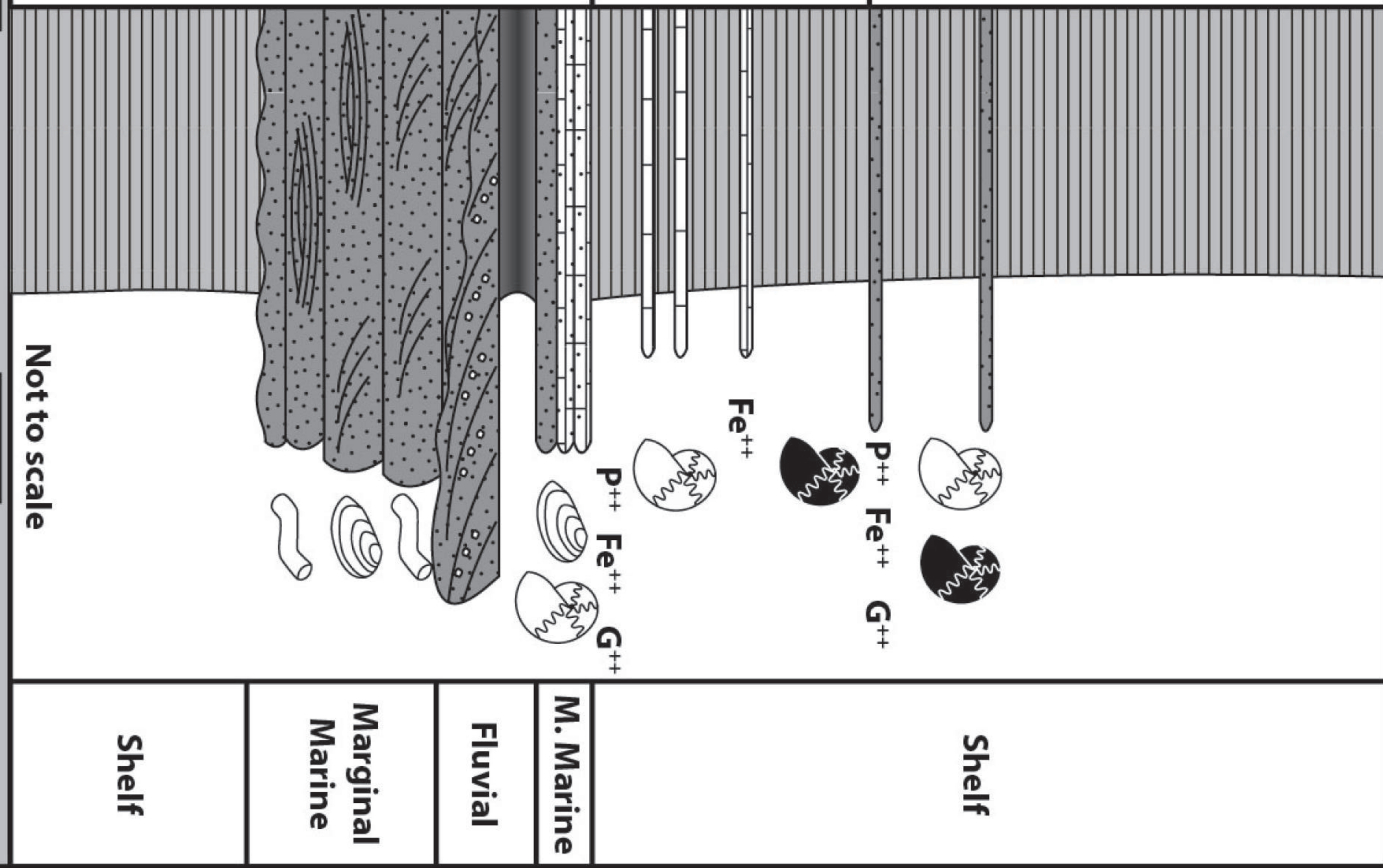

Substage | Format. | Ammon. Zone | Ammon. Subzone | Height (m) | Bed Nr. | Clay | Silt | Very fine | Fine | Med | Crs | Very crs | Grav. | Sand | Mudstone | W.st. | Pack/Grainstone | Rud.

l. Alb. p.p. | O.Tid. p.p. | *Tiskatinensis* Zone | *"Hypacanthoplites" spp.* Sz. | 35 | 249 | 248 | 246 | 244 | 242 | 240 | 238 | 236 | 234 | 232 | 230 | 228 | 226 | 224 | 222 | 220 | 218 | 216 | 214 | 212 | 210 | 206 | 204 | 202 | 200 | 198 | 196 | 194 | 192 | 191 | 190 | 188 | 186 | b | 185 | a | 184 | b | 183 | a | 182 | 180 | 178 | 176 | 174 | 172 | 170 | 168 | 166 | c | 165 b | a | 164 | 162 | 161 a | b | 160 a | 160 | 159 | 157 | Barren | Fe⁺ | Ph⁺Gl⁺Fe⁺ | Ph, Fe | D | Fe⁺ | Pyr | Fe⁺ | C | Fe⁺ Large | Fe⁺ | Large | Fe⁺ Large | Fe⁺ | Fe⁺ | B | Fe⁺ | Ph⁺Gl⁺Fe⁺ | Th. | Ph⁺ | Large | Fe⁺ | A | Sk. | Fe⁺ | Oy.

Key
- Ammonite (pyritic)
- Belemnite
- Bioturbation (Skolithos Thalassinoides)
- Phosphate
- Glauconite
- Iron
- Hummocky Cross-strat.
- Inverse-grad.
- Reworked Elements
- Iron nodules
- Bivalves
- Samples Foraminifera
- Calcareous Nannofossil
- Barren

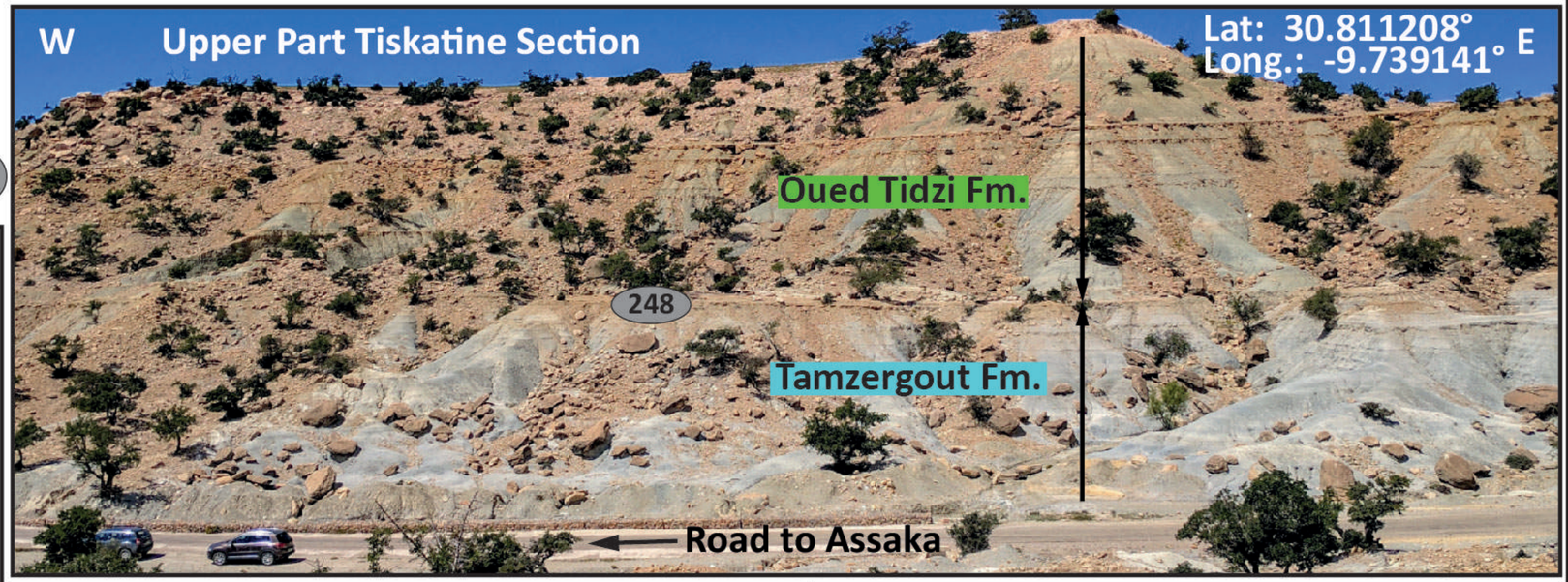

l. Aptian p.p. | upper Aptian | Bouzerg. p.p. | Dechauxi | Tamzergout Fm. | Tobleri Zone | Aschiltaensis Zone | Tob. | Marocanus Subzone

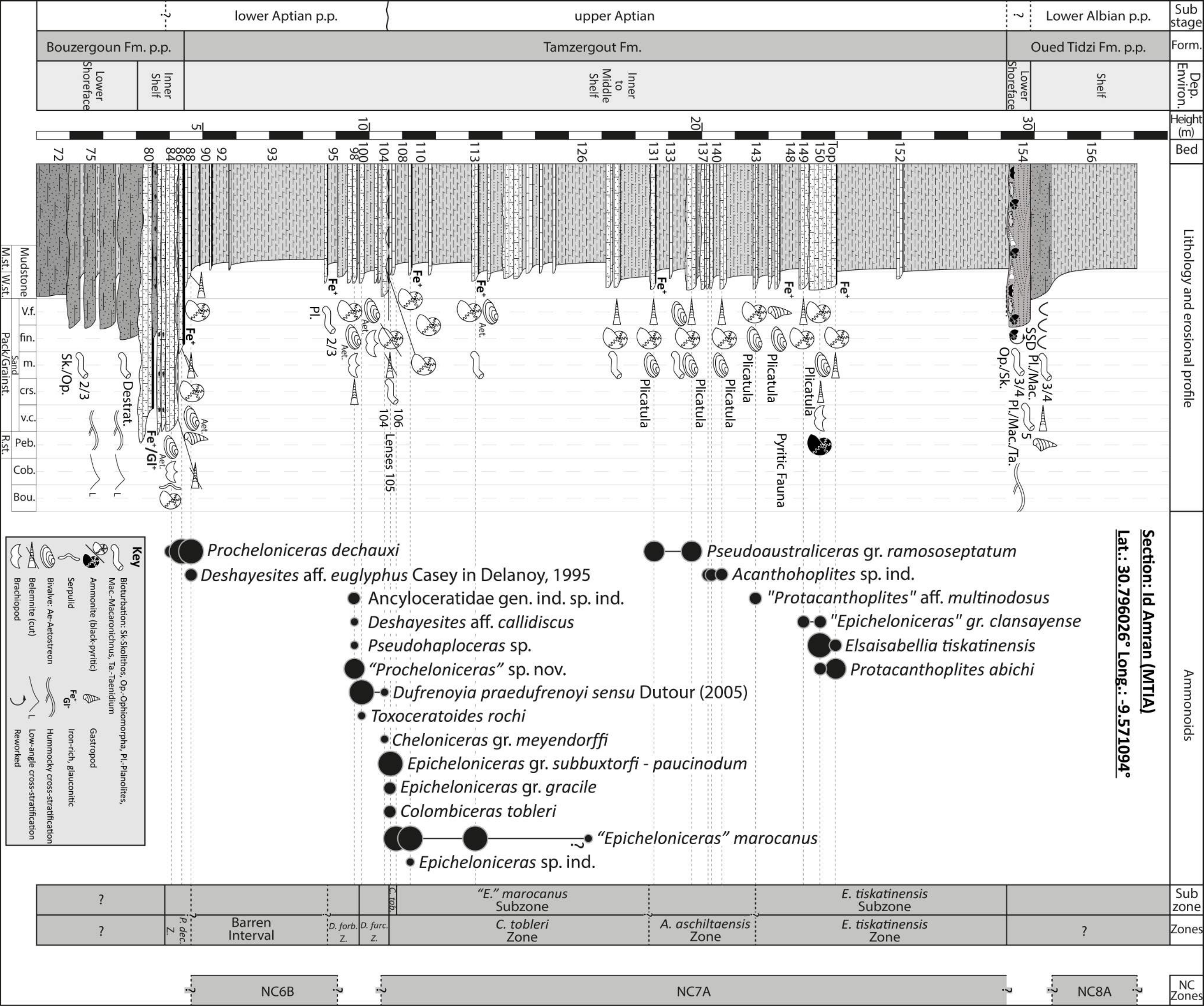

Sub stage
Form.
Dep. Environ.
Height (m)
Bed
Lithology and erosional profile
Ammonoids
Sub zone
Zones
NC Zones
lower Aptian p.p.
upper Aptian
Lower Albian p.p.
Bouzergoun Fm. p.p.
Tamzergout Fm.
Oued Tidzi Fm. p.p.
Lower Shoreface
Inner Shelf
Inner to Middle Shelf
Lower Shoreface
Shelf
Mudstone
M.st.
W.st.
Sand
Pack/Grainst.
R.st.
V.f.
fin.
m.
crs.
v.c.
Peb.
Cob.
Bou.
Sk./Op.
2/3
Destrat.
Fe+/Gl+
Fe+
Aet.
Pl.
2/3
106
104
Lenses 105
Plicatula
Pyritic Fauna
SSD
Pl./Mac.
3/4
Op./Sk.
3/4
Pl./Mac./Ta.
5
Key
Bioturbation: Sk-Skolithos, Op.-Ophiomorpha, Pl.-Planolites, Mac.-Macaronichnus, Ta.-Taenidium
Ammonite (black-pyritic)
Gastropod
Serpulid
Iron-rich, glauconitic
Bivalve: Ae-Aetostreon
Hummocky cross-stratification
Belemnite (cut)
Low-angle cross-stratification
Brachiopod
Reworked
Section: Id Amran (MTIA)
Lat.: 30.796026° Long.: -9.571094°
Procheloniceras dechauxi
Deshayesites aff. euglyphus Casey in Delanoy, 1995
Ancyloceratidae gen. ind. sp. ind.
Deshayesites aff. callidiscus
Pseudohaploceras sp.
"Procheloniceras" sp. nov.
Dufrenoyia praedufrenoyi sensu Dutour (2005)
Toxoceratoides rochi
Cheloniceras gr. meyendorffi
Epicheloniceras gr. subbuxtorfi - paucinodum
Epicheloniceras gr. gracile
Colombiceras tobleri
"Epicheloniceras" marocanus
Epicheloniceras sp. ind.
Pseudoaustraliceras gr. ramososeptatum
Acanthohoplites sp. ind.
"Protacanthoplites" aff. multinodosus
"Epicheloniceras" gr. clansayense
Elsaisabellia tiskatinensis
Protacanthoplites abichi
"E." marocanus Subzone
E. tiskatinensis Subzone
C. tobleri Zone
A. aschiltaensis Zone
E. tiskatinensis Zone
Barren Interval
P. dec. Z.
D. forb. Z.
D. furc. Z.
C. tob.
NC6B
NC7A
NC8A

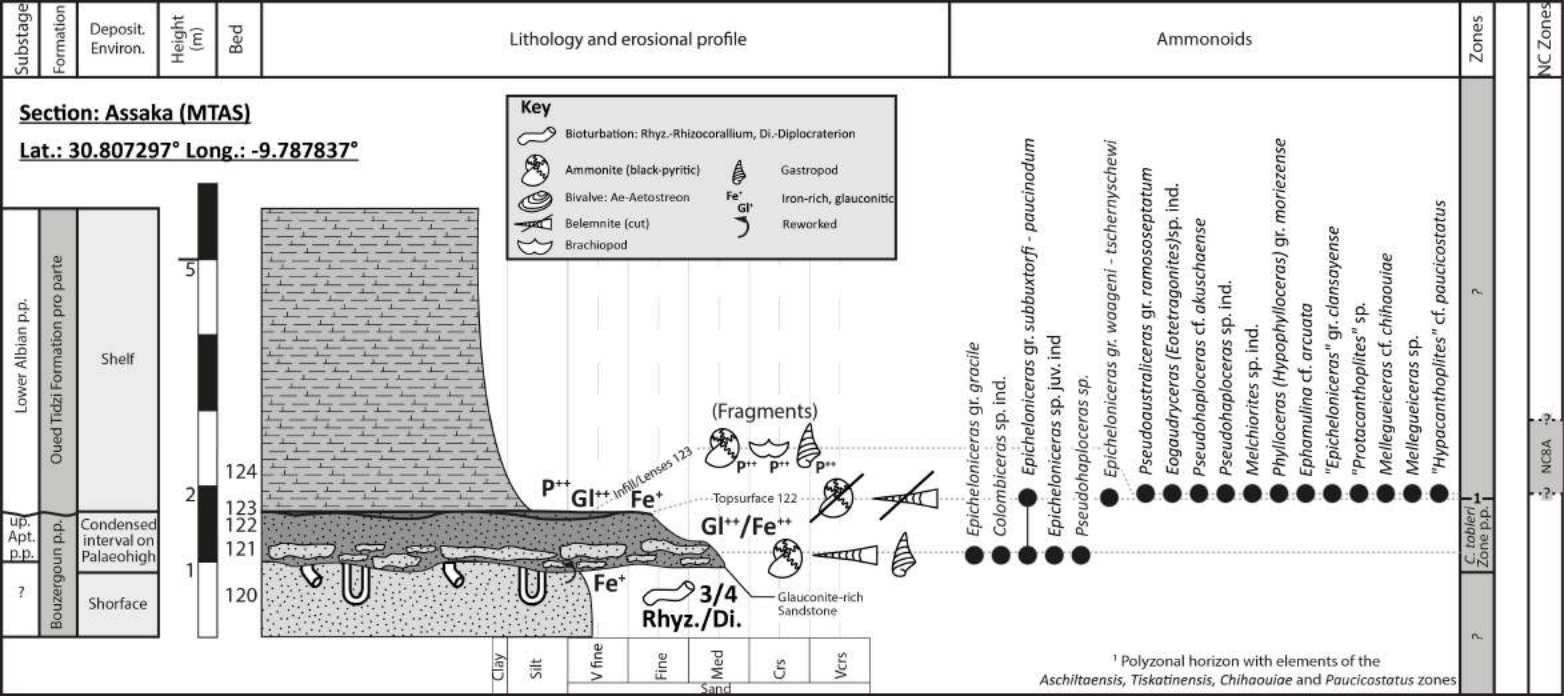
Substage
Formation
Deposit. Environ.
Height (m)
Bed
Lithology and erosional profile
Ammonoids
Zones
NC Zones
Section: Assaka (MTAS)
Lat.: 30.807297° Long.: -9.787837°
Key
Bioturbation: Rhyz.-Rhizocorallium, Di.-Diplocraterion
Ammonite (black-pyritic)
Bivalve: Ae-Aetostreon
Belemnite (cut)
Brachiopod
Gastropod
Fe+ Iron-rich, glauconitic
Gl* Reworked
Lower Albian p.p.
Oued Tidzi Formation pro parte
Shelf
up. Apt. p.p.
Bouzergoun p.p.
Condensed interval on Palaeohigh
?
Shorface
5
2
1
124
123
122
121
120
P++ Gl++ Fe+ infill/Lenses 123
Topsurface 122
Gl++/Fe++
Fe+
3/4 Rhyz./Di.
(Fragments)
Glauconite-rich Sandstone
Epicheloniceras gr. gracile
Colombiceras sp. ind.
Epicheloniceras gr. subbuxtorfi - paucinodum
Epicheloniceras sp. juv. ind
Pseudohaploceras sp.
Epicheloniceras gr. waageni - tschernyschewi
Pseudoaustraliceras gr. ramososeptatum
Eogaudryceras (Eotetragonites)sp. ind.
Pseudohaploceras cf. akuschaense
Pseudohaploceras sp. ind.
Melchiorites sp. ind.
Phylloceras (Hypophylloceras) gr. moriezense
Ephamulina cf. arcuata
"Epicheloniceras" gr. clansayense
"Protacanthoplites" sp.
Mellegueiceras cf. chihaouiae
Mellegueiceras sp.
"Hypacanthoplites" cf. paucicostatus
C. tobleri Zone p.p.
?
1
NC8A
Clay
Silt
V fine
Fine
Med
Crs
Vcrs
Sand
[1] Polyzonal horizon with elements of the Aschiltaensis, Tiskatinensis, Chihaouiae and Paucicostatus zones

DSDP Leg 41 - Borehole 370
Core 34 Section 1 - Core 32 Section 3

Stages: Albian p.p. / Aptian p.p. / Barremian p.p.
Sub-Stages: Lower Albian p.p. / lower Aptian p.p. / upper Barr. p.p.

Well depth (BML) & Core Section

837.5 m
- 5029284
- 32-3
- 5026904
- 5029286

839.0 m
- 5026905
- 5029298
- 32-4
- 5029295
- 5029299
- 5029296
- 5029300
- 5029297
- 5026906

840.5 m
- 5029485
- 5029303
- 5029486
- 5029302
- 34-1
- 5026907
- 5029301

874.0 m

3/4 Ch.
2/3 Ch.
1/2 Ch.
4/5 Ch./Pa.
2/3 Pa.
S+
3/4 Pa./Ch.?
3/4 Ch.
Void
Colour Change: Grey / Green
Chlorite?/G+
Colour Change: Green / Grey
3/4 Ch./Pl.
S+
Void
Gap for 32.0 m
including: CC 33, Core 33, 9.5m Gap, CC 32, 3.5 m Gap
Void

Lithology: Mud | Sand (V.f. fine med crs V.c.) | Pebble | Cobble | Boulder

Calcareous Nannofossils

NC Zone: NC 8A / Barren Interval / NC 6B / Barren Interval / Gap / NC 6A

- P. columnata
- R. achlyostaurion
- C. margerelii ■
- A. terebrodentarius ■
- A. terebrodentarius ssp. youngii
- P. furtiva
- Z. scutula
- (Absence: Nannoconus spp.)
- C. rothii
- N. steinmannii ← F. oblongus

Lithologies/Appearance: Marl; Limestone; Sandstone; Sandy Limestone; Argillaceous Sandstone; Sandy Marl / Calc. Sst; Non-calc. Mudstone; Cross bedded Sst; Pebble-bearing cross bedded Sst; Rippled or wavy bedded Sst; Nodular appearance; Breccia

Sedimentary Structures: Ripples; Cross bedding; Low-angle foresets; Teepee structures; Convolute Bedding; Mud rip ups; Lamination; HCS; Dewatering/SSD; Mudcracks; Pebble-bearing; Nodules; Sample taken; Sed. Intraclast; Injectite

Minerals: G+ Glauconite; P+ Phosphate; Fe+ Iron-Oxides; S+ Sulfates

Bioturbation: Pl Planolites; Pa Palaeophycus; Ch Chondrites

Fossils: Sponges; Algae; Wood fragments; Bivalves; Bioturbation; Ooids; Belemnite; Plant fragm.; Coal fragm.; Gastropodes; Echinoderms; Shells unident.; Ammonite / Nautilus (N); Serpulids; Brachiopods; Foraminifera; Fish Teeth; Rudist; Foraminifera (benthic)

1: very rare; 2: rare; 3: common; 4: abundant; 5: very abundant

DSDP Leg 41 - Borehole 370
Core 32 Section 2 - Core 31 Section 4

Stages: Albian p.p.
Sub-Stages: Lower Albian p.p.

Well depth (BML) & Core Section

829.5 m
- 5029211
- 31-4
- 5029229
- 5029230
- 5029239
- 5029231
- 5026902

831.0 m

834.5 m
- 32-1

836.0 m
- 5029243
- 5029263
- 32-2
- 5029264
- 5029265

837.5 m

3/4 Ch./Pl.
Colour Change: Grey / Green
Colour Change: Green / Grey
4/5 Ch./Pl.
Expanded Core
Gap for 3.5 m
Void for 0.76 m
4/5 Ch./Pl.

Lithology: Mud | Sand (V.f. fine med crs V.c.) | Pebble | Cobble | Boulder

Calcareous Nannofossils

NC Zone: NC 8A

- C. bosunensis
- A. terebrodentarius ssp. youngii
- P. columnata
- R. achlyostaurion
- R. parvidentatum Influx

Species range EAB (this study)

Period	Stage	Sub-Stage	Foraminifera Zonation (Premoli and Verga, 2004)	H. trochoidea	G. ferreolensis	G. barri	G. algerianus	P. cheniourensis	P. bejaouensis	Zones (EAB) (Luber et al. 2017)	Subzones (EAB) (Luber et al. 2017)	Zones (SMAS) (Reboulet etal., 2011, 2014)
Cretaceous	Albian	Low. p.p.	*H. planispira p.p.* (not observed)							*M. chihaouiae*		*L. tardefurcata*
										Hiatus		*H. jacobi*
	Aptian	upper	*H. trochoidea - P. bejaouensis*						●?	*E. tiskatinensis*	*"Hypacanthoplites" spp.*	*N. nolani*
											E. tiskatinensis	
		lower p.p.	*G. algerianus*							*A. aschiltaensis*		*P. melchioris*
			G. ferreolensis							*C. tobleri*	Barren Interval	*E. martini*
											"E." marocanus	
											C. tobleri	
			L. cabri p.p. (not observed)							*Hiatus*		*D. furcata* p.p.

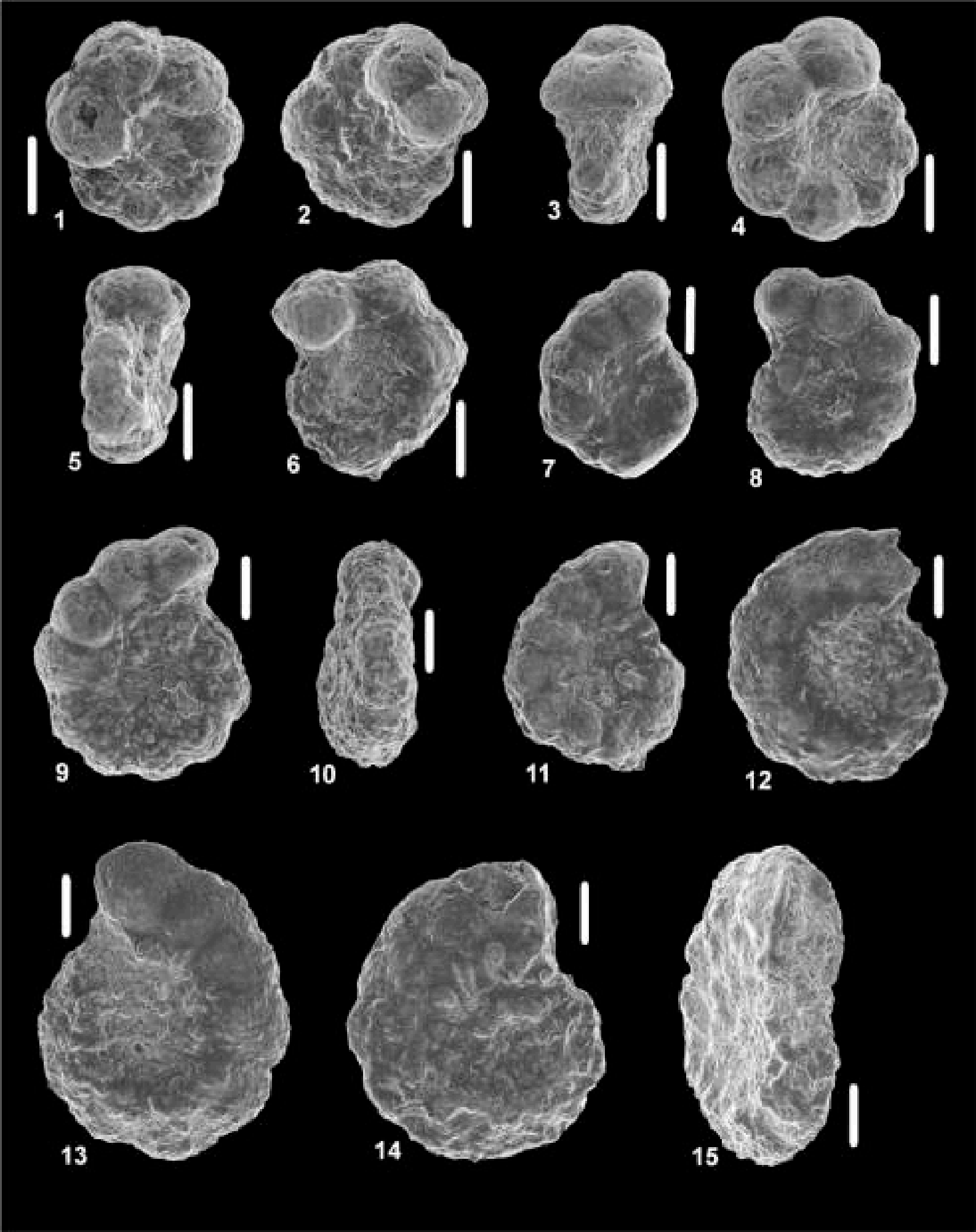
1
2
3
4
5
6
7
8
9
10
11
12
13
14
15

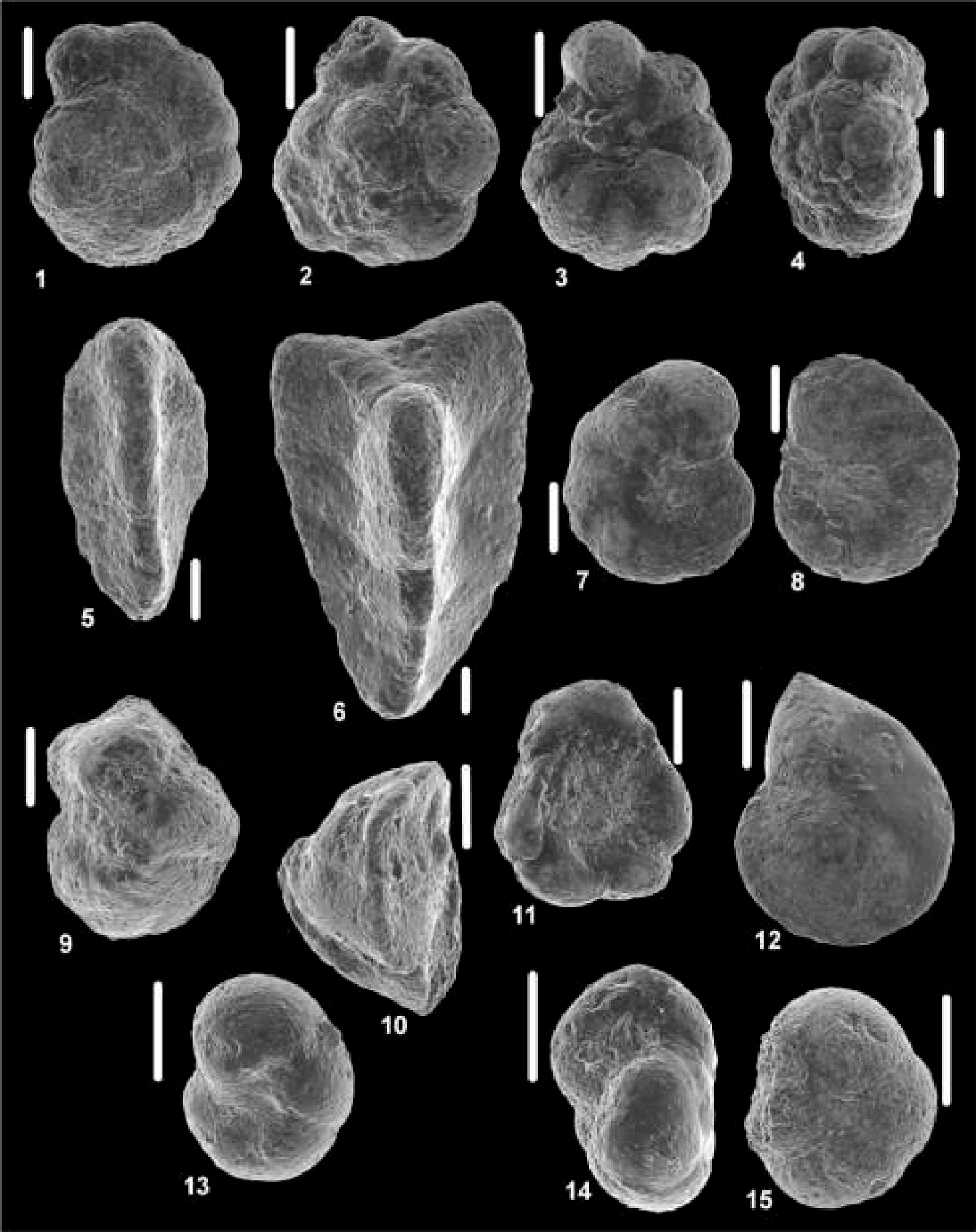
1
2
3
4
5
6
7
8
9
10
11
12
13
14
15

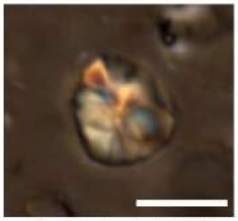

Assipetra terebrodentarius
DSDP 370: 840.03m

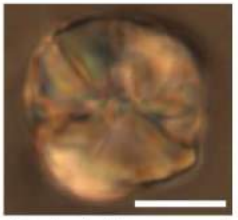

A. terebrodentarius ssp. youngii
Id Amran: MTIA-98

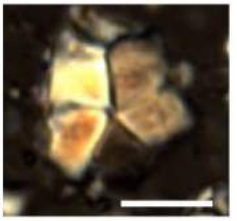

Braarudosphaera africana
Tiskatine MTTK-171

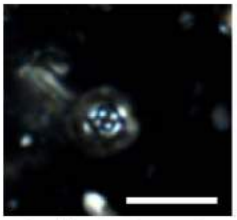

Crucibiscutum bosunensis
Tiskatine MTTK-171

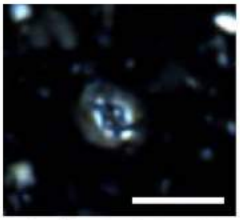

Crucibiscutum bosunensis
Id Amran: MTIA-153

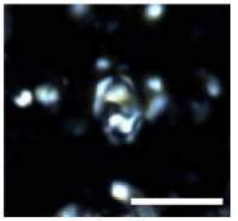

Calculites dispar
Tiskatine: MTTK-171

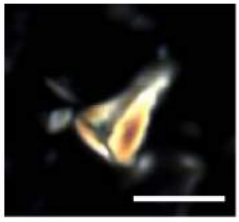

Calculites dispar (side view)
Tiskatine: MTTK-171

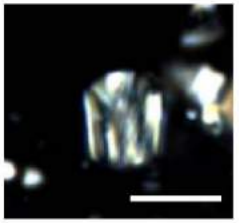

Conusphaera rothii
DSDP 370: 873.98m

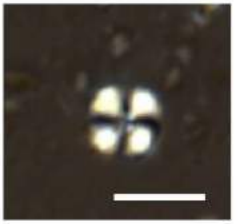

Cyclagelosphaera margerelii
Id Amran: MTIA-98

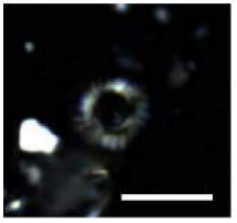

Diazomatolithus lehmanii
DSDP 370: 873.98m

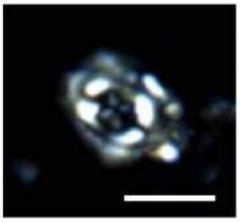

Flabellites oblongus
Id Amran: MTIA-98

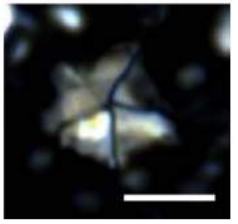

Micrantholithus hoschulzii
Id Amran: MTIA-98

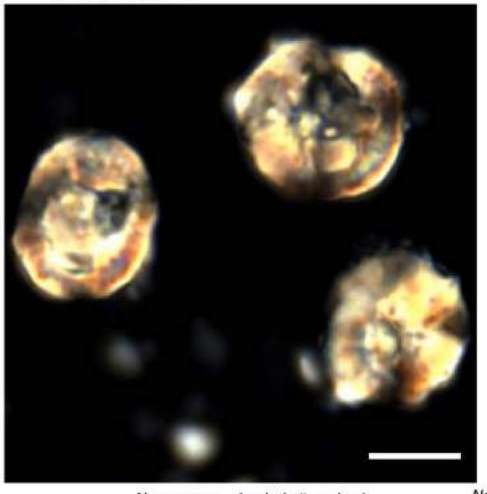

Nannoconus circularis (top view)
Id Amran: MTIA-98

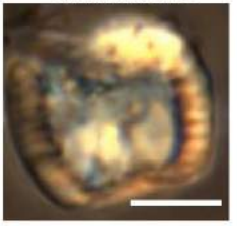

Nannoconus circularis
Id Amran: MTIA-97

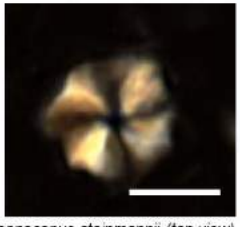

Nannoconus steinmannii (top view)
DSDP 370: 874.81m

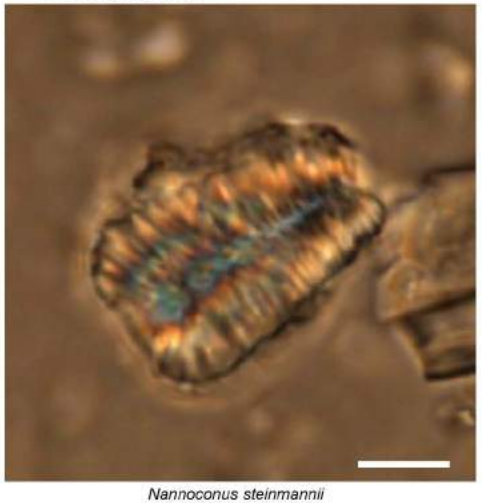

Nannoconus steinmannii
DSDP 370: 874.81m

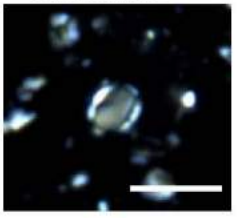

Orastrum perspicuum
Tiskatine: MTTK-171

Prediscosphaera columnata
DSDP 370: 811.95m

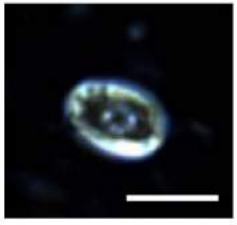

Rhagodiscus achlyostaurion
DSDP 370: 811.95m

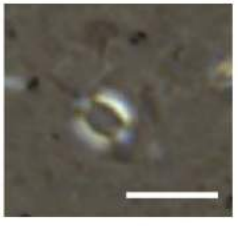

Repagulum parvidentatum
DSDP 370: 811.95m

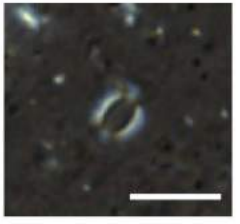

Repagulum parvidentatum
DSDP 370: 811.95m

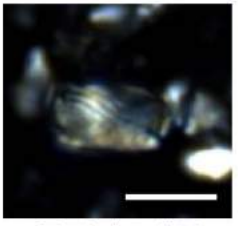

Zebrashapka vanhintei
Id Amran: MTIA-153

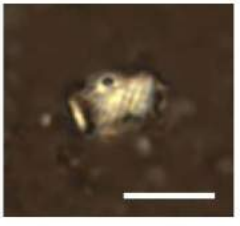

Zebrashapka vanhintei
Id Amran: MTIA-153

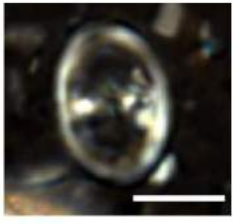

Zeugrhabdotus scutula
DSDP370: 873.98m

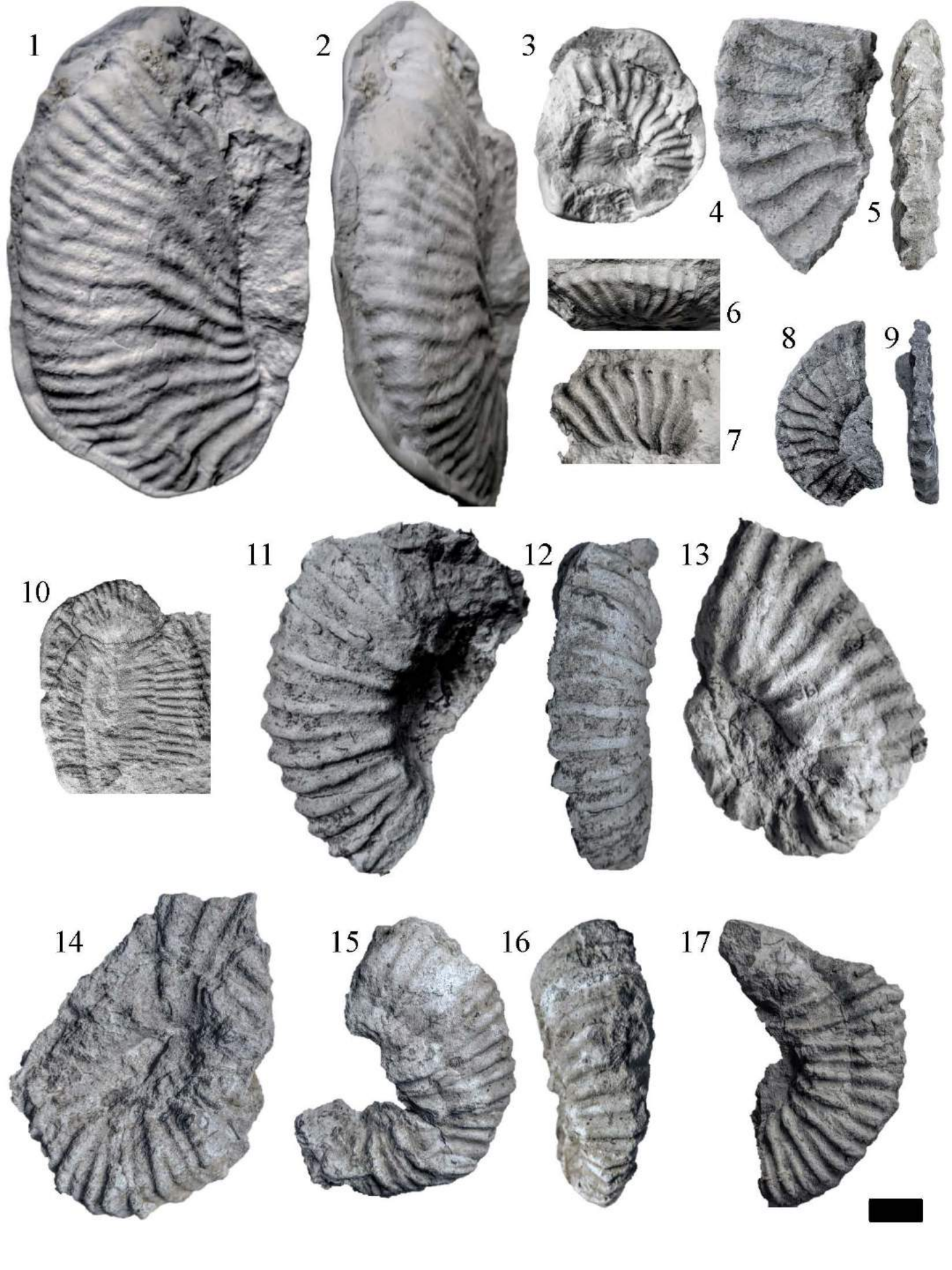
1
2
3
4
5
6
7
8
9
10
11
12
13
14
15
16
17

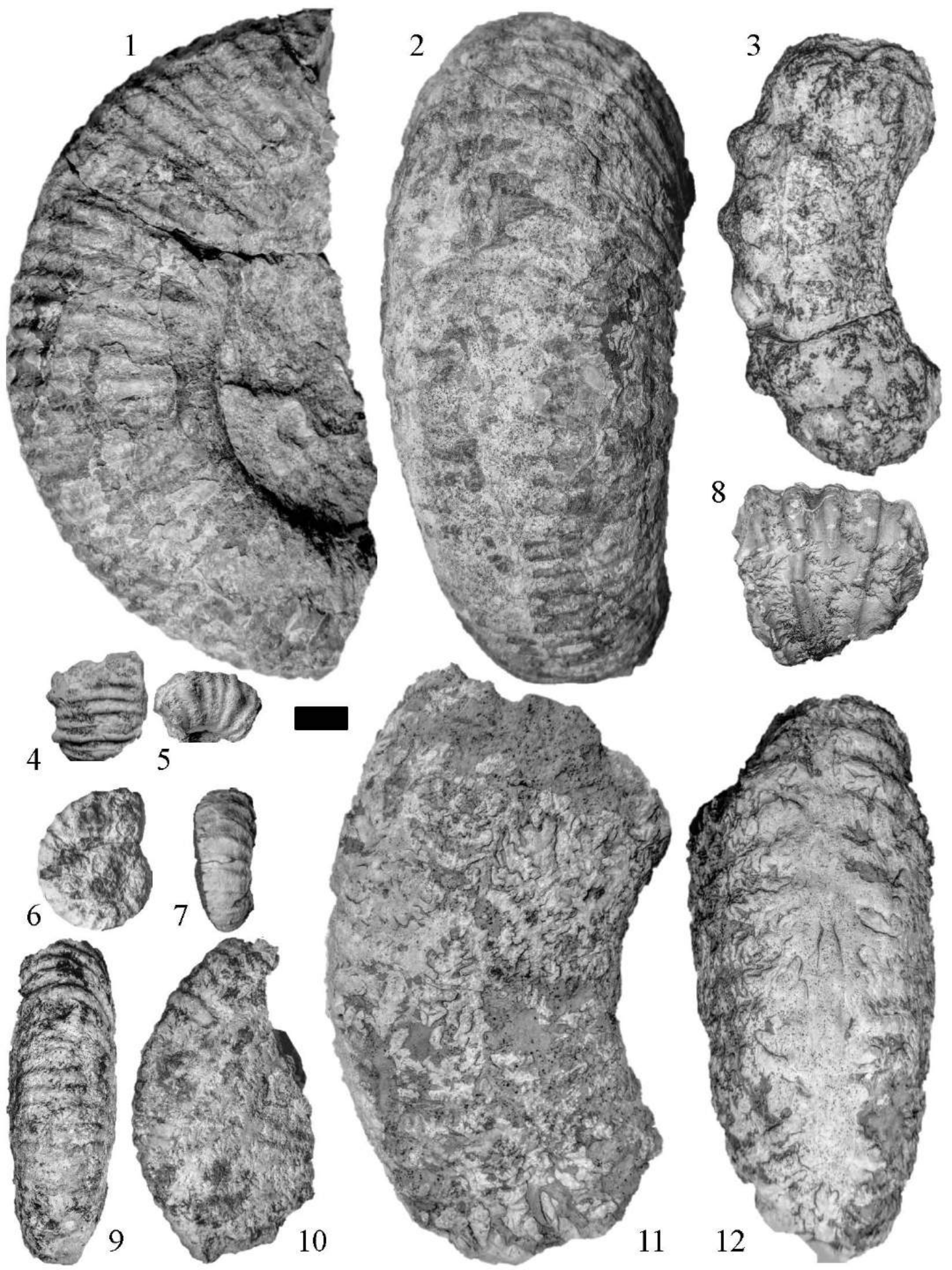
1
2
3
8
4
5
6
7
9
10
11
12

Substage	Formation	Height (m)	Bed	Lithology and erosional profile	Ammonoids	Subzone	Zone	Zone	Planktonic Foraminifera	Benthonic Foraminifera	Ratio of planktonic, benthonic and agglutinating benthonic foramnifera	Sub-Zone	Nannofossils	Sequence Stratigraphic Events
L. Alb. p.p.	Oued Tidzi p.p.				*D. leightonense*		*M. chihaouiae* Z. p.p.	ind.	?*P. bejaouaensis* *G. ferreolensis* & *H. trocoidea*	*Ga.* cf. *barremiana* Influx eroded *E. ex* gr. *ornata*	0% 50% 100%	NC8A p.p.	*Holococcoliths* (HRA) including: *O. perspicuum*, *O. partitum* and *C. dispar* *P. columnata* & *R. achlyostaurion* & *R. parvidentatum* (HRA)	basal Albian sequence boundary
upper Aptian	Tamzergout Fm.	35	249 (17) 248 245 243 241 239 237 235 233 231 229 227	Fe+ Ph+ Gl+ Fe+ Pyr Ph Fe+ Pyr Fe+	*Diadochoceras* & *"Hypacanthoplites"* spp.	*"Hypacanthoplites"* spp. Subzone	*E. tiskatinensis* Zone	*H. trocoidea* - *P. bejaouensis* Zone (undiffer.)	*P. cheniourensis*	*T.*? *dividens*	Influx eroded *E.* ex gr. *ornata*	NC7 und.	*Nannoconus* spp.■ incl.: *N. fragilis*, *N. quadriangulus* *C. bosunensis* & *Z. vanhintei* & *O. perspicuum* ■ *A. terebrodentarius youngii* & *M. hoschulzii* ← Acme *C. bosunensis*	
		30	225 223 221 219 217 215 (8)213 211 209	Fe+	*"Hypacanthoplites"* spp.									
		25	(5) 206 205 204 203 201 199 197	Fe+ Fe+	*Diadochoceras*	*E. tiskatinensis* Sz.			*P. cheniourensis* *Gl. barri*					upper Aptian Maximum Flooding
		20	195 192 191 189 187	Fe+ Large Fe+ Large Fe+ Large	*A. aschiltaensis*		*A. aschiltaensis* Zone	*Gl. algerianus* Zone	*Gl. algerianus* *H. trocoidea*			NC7A p.p.		
		15	b 185 a 184 b 183 a	Fe+	*A. aschiltaensis*	*"E." marocanus* Subzone	*C. tobleri* Zone	*Gl. ferreolensis* Zone	*Gl. barri* *Gl. algerianus-ferreoloensis* (transitional forms)	*T.*? *dividens* & Influx eroded *E.* ex gr. *ornata*				
		10	182 179 177 175 173 171 169	*Epicheloniceras*										
		5	166 c 165m a 164 162top 161 a 160 b 160 a 160 159	Fe+ Ph+ Gl+ Fe+ Pyr Ph Ph+ Fe+ Large	*C. tobleri* *Epicheloniceras* & *C. tobleri* *P. dechauxi* & *D.* aff. *euglyphus* *D.* aff. *euglyphus* *P. dechauxi*	*C. tob.*	*P. Dechauxi* Zone		*Gl. ferreolensis*	*Ga.* cf. *barremiana*	*Holococcoliths* (HRA) *S. achylosus* & *Z. vanhintei*		*Holococcoliths* (HRA) *S. achylosus* & *Z. vanhintei*	lower upper Aptian Maximum Flooding
l. Apt. p.p.	Bouzergoun p.p.		157	Fe+ Oyster				Barren Interval			Barren	Not Studied		lower/upper Aptian Sequence Boundary

Substage | Formation | Height (m) | Bed | Lithology and erosional profile | Carbonate Content | TOC | $\partial^{13}C_{carb}$ | $\partial^{13}C_{org}$ | EAB Ammo. SZ. | EAB Ammo. Z. | SMAS Z. | Foraminif. Zone | Calc. Nan. Sub-Zone

L. Alb. p.p. | O. Tidzi p.p.

basal Albian Unconformity

Diagenetically altered Zone

$\partial^{13}C_{carb}$ Peak 2

$\partial^{13}C_{carb}$ Peak 1

Diagenetically altered Zone

lower/upper Aptian Boundary Unconformity

upper Aptian | Tamzergout Fm.

l. Aptian p.p. | Bouzergoun p.p.

M. chihaouiae Z. p.p. | *L. tarde.* Z. p.p. | ind. | NC8A p.p.

"*Hypacanthoplites*" spp. Subzone | *E. tiskatinensis* Sz. | *E. tiskatinensis* Zone | *N. nolani* Zone | *H. trocoidea - P. bejaouensis* Zone | ?

A. aschiltaensis Zone | *P. melchioris* Zone | *Gl. algerianus* Zone | NC7A p.p.

"*E.*" *marocanus* Subzone | *C. tobleri* Zone | *E. martini* Zone p.p. | *Gl. ferreolensis* Zone | Barren

C. tob. | *P. dechauxi* Zone | *D. forbesi* Zone p.p. | Not Studied

Carbonate (%) | TOC (%) | $\delta^{13}C_{carb}$ (‰VPDB) | $\delta^{13}C_{org}$ (‰VPDB)

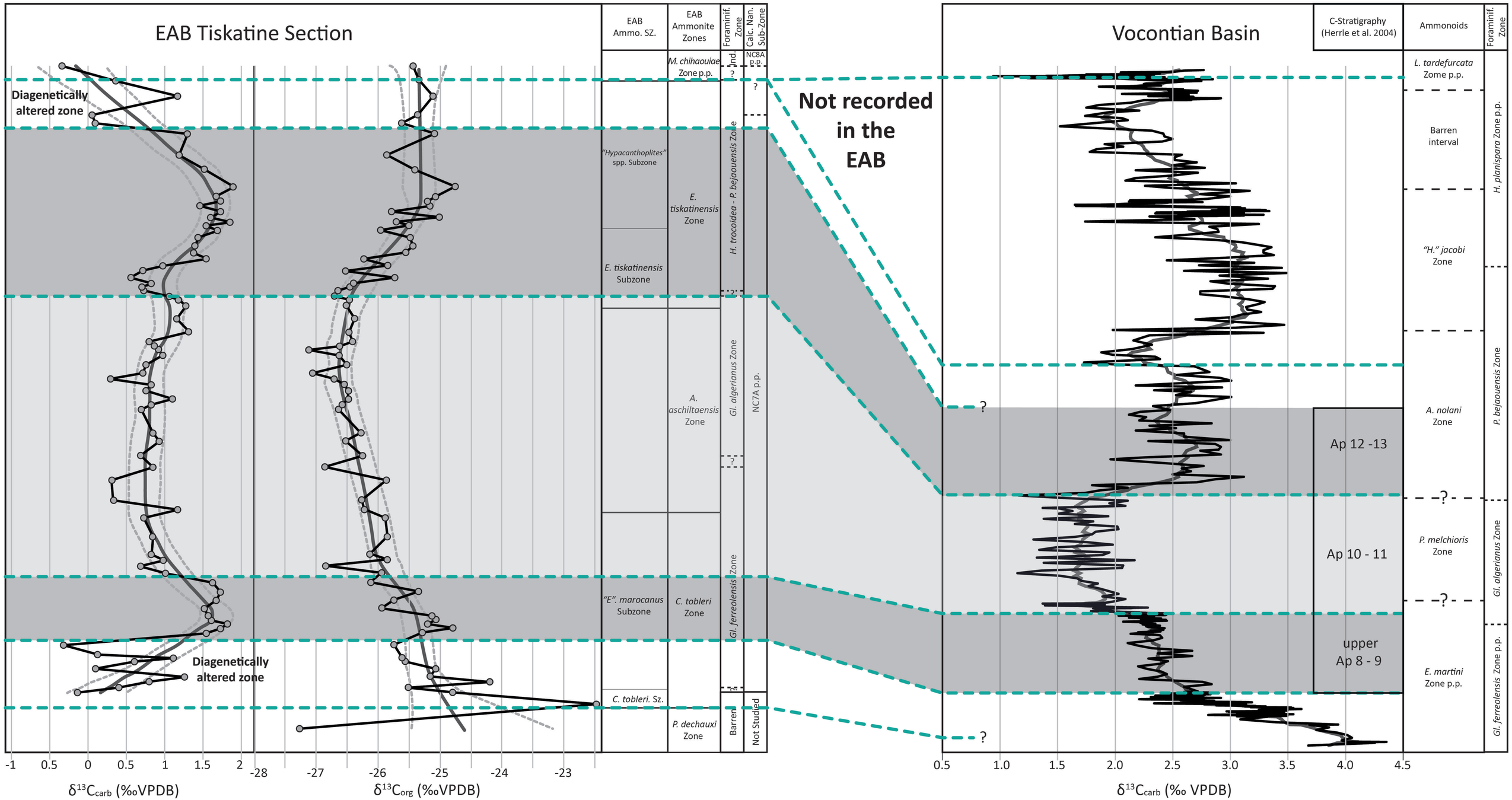
EAB Tiskatine Section
Diagenetically altered zone
Diagenetically altered zone
EAB Ammo. SZ.
EAB Ammonite Zones
Foraminif. Zone
Calc. Nan. Sub-Zone
M. chihaouiae Zone p.p.
Ind.
NC8A p.p.
"Hypacanthoplites" spp. Subzone
E. tiskatinensis Zone
E. tiskatinensis Subzone
H. trocoidea - P. bejaouensis Zone
A. aschiltaensis Zone
Gl. algerianus Zone
NC7A p.p.
"E". marocanus Subzone
C. tobleri Zone
Gl. ferreolensis Zone
C. tobleri. Sz.
P. dechauxi Zone
Barren
Not Studied
Not recorded in the EAB
Vocontian Basin
C-Stratigraphy (Herrle et al. 2004)
Ammonoids
Foraminif. Zone
L. tardefurcata Zone p.p.
Barren interval
"H." jacobi Zone
A. nolani Zone
P. melchioris Zone
E. martini Zone p.p.
H. planispara Zone p.p.
P. bejaouensis Zone
Gl. algerianus Zone
Gl. ferreolensis Zone p.p.
Ap 12 -13
Ap 10 - 11
upper Ap 8 - 9
-1 0.5 0 0.5 1 1.5 2
δ13Ccarb (‰VPDB)
-28 -27 -26 -25 -24 -23
δ13Corg (‰VPDB)
0.5 1.0 1.5 2.0 2.5 3.0 3.5 4.0 4.5
δ13Ccarb (‰ VPDB)

W

E

7 Km

13 Km

Assaka

Tiskatine

Id Amran

3 Oued Tidzi Fm.

2 Tamzergout Fm.

1 Bouzergoun Fm.

Siliciclastic-dominated

Limestone-dominated

Marl (blue)-dominated

Marl (green)-dominated

SB

FO: *Douvilleiceras*

LO: *E. tiskatinensis*

FO: *E. tiskatinensis*

FO: *Pseudoaustraliceras*

FO: *D. furcata*

FO: *C. tobleri*

FO: "*E.*" *marocanus*

LO: *P. dechauxi*

FO: *P. dechauxi*

Plicatula

Pyritic Fauna

Destrat.

Sk./Op.

10 m

SB

Hiatus

MFS

SB

Hiatus

MFS

SB

Hiatus

MFS

Movement phases on palaeotopographic high

Duration of Zones [Ma]	Zones (SMAS)	Stages		Zones (EAB)
	L. tard. p.p.	L. Albian p.p.	Albian	*M. chlh.* p.p.
2.5	*H. jacobi* Zone	upper Aptian	Aptian	
1.15	*N. nolani* Zone			*E. tiskatin.* Zone
1.13 - 1.35	*P. melchioris* Zone			*A. aschiltaensis* Zone
0.6	*E. martini* Zone			*C. tobleri* Zone
1.0				
0.6	*D. furca.* Zone	lower Aptian p.p.		*D. fur.*
0.6	*D. desha.* Zone			
0.5	*D. forbesi* Z. p.p.			*D. for.* *P. dec.*
?				
?				